

Adaptive event-triggered pinning synchronization control for complex networks with random saturation subject to hybrid cyber-attacks

M. Syed Ali¹  | M. Mubeen Tajudeen¹ | Grienggrai Rajchakit² | Bandana Priya³ | Ganesh Kumar Thakur⁴

¹Complex systems and Networked Science Lab, Department of Mathematics, Thiruvalluvar University, Vellore, Tamil Nadu, India

²Department of Mathematics, Faculty of Science, Maejo University, San Sai, Chiang Mai, Thailand

³Department of Applied sciences and Humanities, G L Bajaj Institute of Technology and Management, Greater Noida, Uttar Pradesh, India

⁴Department of Applied sciences and Humanities, ABES Engineering College, Ghaziabad, Uttar Pradesh, India

Correspondence

Grienggrai Rajchakit, Department of Mathematics, Faculty of Science, Maejo University, San Sai, 50290, Chiang Mai, Thailand.

Email: kreangkri@mju.ac.th

Funding information

National Research Council of Thailand, Grant/Award Number: N42A650250

Summary

This research is concerned with the problem of pinning based output synchronization control for a complex networks with random saturation vulnerable to hybrid cyber-attacks via an adaptive event-triggered scheme (AETS). The output synchronization error systems are subject to suffer from deception attacks, replay attacks, and denial-of-service attacks. A novel hybrid cyber-attack model is first constructed to integrate the three kinds of attacks into a synchronization of complex network. AETSs based on output synchronization errors with the consideration of hybrid cyber-attacks, have been proposed to reduce the burden of communication. A pinning control strategy is used to decrease the control signal's input. By constructing a Lyapunov functional and using the linear matrix inequality technique, sufficient conditions are provided to ensure the output synchronization error system. Finally, a numerical simulation results are developed to illustrate the efficacy of the proposed theoretical methodology.

KEYWORDS

adaptive event-triggered pinning control, complex networks, hybrid attacks, Lyapunov-functional

1 | INTRODUCTION

Complex networks (CNs) have gotten a lot of attention in recent years because of their variety of applications, including biological systems, communications networks, World Wide Web, electric power grids, and robot formation.¹⁻³ Numerous researchers have devoted decades to the study of complex dynamical networks (CDNs), particularly in the domain of synchronization.^{4,5} The phenomenon of synchronization is common among the dynamical behaviors of CNs. In the past few years, this essential and interesting collective behavior in CNs has received a lot of attention for its wide range of applications. For instance, communication security, biological networks, ecosystems, chaos-based communication networks, parallel image processing.⁶⁻⁹ As a result, the synchronization of CNs has become a popular issue in both principles and applications. Many significant results in the synchronization of various CDNs have been reported so far.¹⁰⁻¹³ Some appropriate controllers must be designed in order to drive a complex dynamic network to achieve synchronization. Recently, different control techniques for synchronizing CDNs have been developed, including fault-tolerant control,¹⁴ sampled-data control,¹⁵ impulsive control,¹⁶ pinning control,¹⁷ and adaptive control. In Reference 5, some necessary requirements for establishing pinning synchronization on CNs are described.

In CNs, control strategy is always an interesting topic. The time-triggered scheme, in which sampled data is transferred to the communication network at a fixed time interval, has been the most widely used transmission technique in recent decades.¹⁸ An event-triggered mechanism was developed and is widely used to reduce unnecessary resource consumption.¹⁹ One of the most difficult aspects of implementing event-triggered control (ETC) is that the event function must be continuously monitored, which is difficult to achieve on digital platforms. The control cost can be significantly reduced with the implementation of this triggering mechanism. As a result, ETC has been widely used to research CNs, multi-agent systems, logical control systems, and biological systems.²⁰⁻²² To address the interactions between the quantifier and the sampler, novel event-triggering and quantization mechanisms were proposed in References 23 and 24. The adaptive ETC strategy is used to output feedback control, thereby resolving the problem of unmeasurable states.²⁵⁻²⁹

As we all know, the saturation is a frequently encountered event, caused by physical constraints in many practical applications.³⁰⁻³² The presence of saturation nonlinearity can reduce the performance of systems and potentially cause them to become unstable. This can lead to adverse performance degradation. As a result, the challenge of saturation analysis and control deserves a huge amount of attention.³³ Even if the input is known, we can't get the outputs with direct feed through because of output saturation.^{34,35}

With the advancement of networks and modern technology, cyber security has recently become more essential. As a result,³⁶ there has been a strong interest in investigating the impact of various cyber-attacks on CNs. In particular, cyber-attacks have been considered a leading challenge to network security, with the goal of disrupting control performance and degrading stability by destroying critical data transmitted across a network.³⁷ Cyber-attacks are classified into three kinds: deception attacks,³⁸ replay attacks,³⁹ and denial of service (DoS).⁴⁰ Numerous researchers have focused on the issue of system control synthesis under cyber-attacks.^{38,41-43} By preventing the signal or information from reaching its desired target, DoS attacks damage the system's performance. Deception attacks occur when attackers may introduce false data into actual data, destroying the integrity of the data. Secure synchronization of CNs under deception attacks against vulnerable nodes.³⁸ A replay attack is a special type of deception attack in which the attacker can access, record, and replay sensor data. In Reference 40, adaptive control design is used to guarantee the security and safety of sensor and actuator attacks. The decentralized event-triggered H_∞ control system under cyber-attacks is addressed in References 41,44-46.

Based on the preceding results, this article studies the pinning based output synchronization control problem for CNs with random saturation subjected to hybrid cyber-attacks via adaptive event-triggered scheme (AETS). To the best of authors knowledge, pinning synchronization of CNs with hybrid cyber attacks have not been studied yet. To be more specific, the following are the main features of this work:

1. To begin, we changed the output pinning synchronization problem of master-slave CNs into the stability problem of the synchronization error system while simultaneously considering hybrid cyber-attacks and random saturation.
2. In the previous work^{11,12,38} either DoS or deception or both attacks are considered, but in this article a novel unified framework of hybrid attacks is proposed in synchronization of CNs, which considers deception attacks, replay attacks, and DoS attacks at the same time, in contrast to the existing works. In reality, this attack technique is widely available, specifically in complex dynamical systems.
3. A novel output pinning synchronization control based on AETS is proposed, which can reduce computational load and preserve communication resources. In comparison to previous studies,^{13,46} proposed control is more realistic and advantageous for saving communication resources.
4. Novel sufficient asymptotic stability conditions for synchronization error systems have been established. Event-triggered parameter and the controller gains can be acquired simultaneously utilizing LMI technology.
5. Finally, two numerical examples are presented to demonstrate the proposed design approach's efficiency and superiority.

2 | SYSTEM DESCRIPTION

We consider the following drive system of CNs with N identical nodes:

$$\begin{cases} \dot{\eta}_i(\varphi) = C_i \eta_i(\varphi) + \mathfrak{h}(\eta_i(\varphi)) + \alpha_i \sum_{j=1}^N g_{ij} \Lambda \omega_j(\varphi), \\ \omega_i(\varphi) = D_i \eta_i(\varphi), \quad i = 1, 2, \dots, N, \end{cases} \quad (1)$$

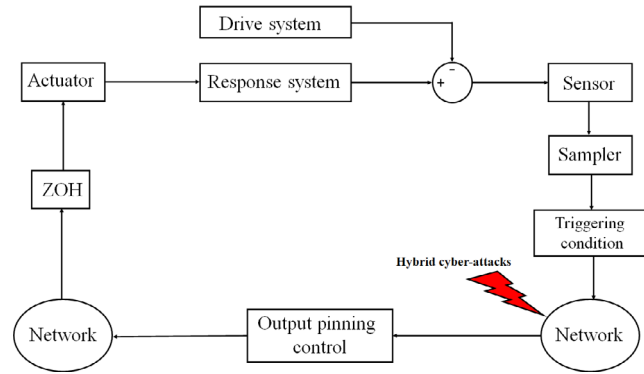


FIGURE 1 Synchronization of complex network under hybrid cyber attacks.

where $\omega_i(\varphi)$ and $\eta_i(\varphi)$ are stands for the output and state of the i th node, at time φ respectively. Coupling strength is denoted by α_i , where $\alpha_i > 0$ and $\mathfrak{h}(\eta_i(\varphi))$ is a nonlinear function. Inner-coupling matrix is denoted by Λ . $G = [g_{ij}]_{N \times N}$ are the external coupling matrices of the network with $g_{ij} > 0$. Generally, the matrices G are symmetric and satisfy $g_{ij} = -\sum_{j=1, j \neq i}^N g_{ij}$. C_i and D_i are the parameter matrices with proper dimensions.

Based on (1), output dynamic model is described as follows

$$\dot{\omega}_i(\varphi) = \bar{C}_i \omega_i(\varphi) + D_i \bar{\mathfrak{h}}(\eta_i(\varphi)) + \alpha_i \sum_{j=1}^N g_{ij} \bar{\Lambda} \omega_j(\varphi), \quad (2)$$

where $\bar{C}_i = D_i A_i D_i^{-1}$, $\bar{\mathfrak{h}}(\eta_i(\varphi)) = \mathfrak{h}(D_i^{-1} \eta_i(\varphi))$, $\bar{\Lambda} = D_i \Lambda$.

The considered response system of complex network model is described as

$$\begin{cases} \dot{\vartheta}_i(\varphi) = C_i \vartheta_i(\varphi) + \mathfrak{h}(\vartheta_i(\varphi)) + \alpha_i \sum_{j=1}^N g_{ij} \Lambda \varpi_j(\varphi) + b_i u_i(\varphi), \\ \varpi_i(\varphi) = D_i \vartheta_i(\varphi), \quad i = 1, 2, \dots, N, \end{cases} \quad (3)$$

where, $b_i > 0$ means node is pinned, otherwise $b_i = 0$. $u_i(\varphi)$ is the control input of the node i .

According to (3), we have

$$\dot{\varpi}_i(\varphi) = \bar{C}_i \varpi_i(\varphi) + D_i \bar{\mathfrak{h}}(\varpi_i(\varphi)) + \alpha_i \sum_{j=1}^N g_{ij} \bar{\Lambda} \varpi_j(\varphi) + b_i D_i u_i(\varphi).$$

Defining $\xi(\varphi) = \varpi(\varphi) - \omega(\varphi)$, we get the following output synchronization error system

$$\dot{\xi}_i(\varphi) = \bar{C}_i \xi_i(\varphi) + D_i \bar{\mathfrak{h}}(\xi_i(\varphi)) + \alpha_i \sum_{j=1}^N g_{ij} \bar{\Lambda} \xi_j(\varphi) + b_i D_i u_i(\varphi), \quad (4)$$

where $\bar{\mathfrak{h}}(\xi_i(\varphi), \varphi) = \bar{\mathfrak{h}}(\varpi_i(\varphi)) - \bar{\mathfrak{h}}(\omega_i(\varphi))$ (Figure 1).

To effectively reduce the communication burden of the shared network, an AETS is introduced between the sensor and the controller for the node i . h is the sampling period and the released instant is $\varphi_k^i h (k = 0, 1, \dots)$, where φ_k^i is a non-negative integer, $t_0^i h = 0$ is the initial instant.

For the node i , the adaptive event-triggered law is taken as

$$\delta_i^T \Theta_i \delta_i \leq \psi_i(\varphi) \xi_i^T((\varphi_k^i + j)h) \Theta_i \xi_i((\varphi_k^i + j)h), \quad (5)$$

where $\delta_i(\varphi) = \xi_i(\varphi_k^i h) - \xi_i((\varphi_k^i + j)h)$, $\Theta_i > 0$ is the parameter of AETS to be determined later and $\psi_i(\varphi)$ satisfies the following condition

$$\dot{\psi}_i(\varphi) = \frac{\nu_i}{\psi_i(\varphi)} \left(\frac{1}{\psi_i(\varphi)} - \kappa_i \right) \delta_i^T \Theta_i \delta_i(\varphi),$$

where $0 < \psi_i(\varphi) < 1$, $\nu_i > 0$, $\kappa_i > 0$.

Thus, based on the triggering law (5), the next released instant can be determined by the following expression.

$$\varphi_{k+1}^i h = \varphi_k^i h + \min\{lh|\delta_i^T(\varphi)\Theta_i\delta_i(\varphi) > \psi_i(\varphi)\xi_i^T((\varphi_k^i + j)h)\Theta_i\xi_i((\varphi_k^i + j)h)\}. \quad (6)$$

The occurrence of communication delays is unavoidable when signals are transmitted through network channels. Therefore, the transmission delay is also considered in this article, which is coincidence with the engineering practice. Let ϕ_k^i as the communication delay of the node i .

Define $\mathfrak{R}_k = [\varphi_k^i h + \phi_k^i, \varphi_{k+1}^i h + \phi_{k+1}^i]$ and \mathfrak{R}_k can be divided as $\mathfrak{R}_k = \bigcup_{m=1}^{w_i} \beta_m^i$, where

$$\beta_m^i = [\varphi_k^i h + mh - h + \phi_k^{i_{m-1}}, \varphi_k^i h + mh + \phi_k^{i_m}],$$

$$\phi_k^{i_m} = \begin{cases} \phi_k^i, & m \leq w_i - 1, \\ \phi_{k+1}^i, & m = w_i. \end{cases}$$

$\phi_i(\varphi) = \varphi - (\varphi_k^i + j)h$, $\varphi \in \beta_m^i$, then under action of zero-order holder, the actual sensor measurement error can be obtained as follows,

$$\bar{\xi}_i(\varphi) = \xi_i(\varphi_k^i h) = \xi_i(\varphi - \phi_i(\varphi)) + \delta_i(\varphi),$$

where $0 \leq \phi_i(\varphi) \leq h + \max\{\phi_k^i\} = \phi_N^i$.

Remark 1. From (6), it is easily known that the sampling instants of node i are released and transmitted at discrete instant $\varphi_k^i h$. Therefore, the event-triggering interval is not less than the sampling period h , that is, $\varphi_{k+1}^i h - \varphi_k^i h \geq h > 0$, which implies that Zeno behavior is avoided under the adaptive event-triggering scheme (6).

Remark 2. Till recently, great focus has been devoted to References 11-13, highlighting the fact that it addresses all aspects of synchronization of CNs under cyber attacks. Numerous studies have focused on using static output feedback control⁴⁶ and ETC⁴⁷ methods to reduce the number of channels that have been attacked during period. As a result, the output-based pinning synchronization control via AETS strategy described in this article is more practical and effectively reduces the communication overhead when compared to the above methodologies.

Under the randomly happening saturation nonlinearities, the error $\bar{\xi}_i(\varphi)$ can be expressed in terms:

$$\bar{\xi}_i(\varphi) = (1 - o_i(\varphi))\bar{\xi}_i(\varphi) + o_i(\varphi)\rho(\bar{\xi}_i(\varphi)), \quad (7)$$

where $o_i(\varphi) \in [0, 1]$ is a stochastic random variable and satisfy the Bernoulli distribution, $\mathbb{E}\{o_i(\varphi)\} = o_{1i}$, $\mathbb{E}\{(o_i(\varphi) - o_{1i})^2\} = \theta_{1i}^2$. From the Equation (7), it indicates that if $o_i(\varphi) = 1$, then, $\bar{\xi}_i(\varphi) = (1 - o_i(\varphi))\bar{\xi}_i(\varphi) + \rho(\bar{\xi}_i(\varphi))$, saturation happen successfully, which means that the controller suffers from saturation signal. If $o_i(\varphi) = 0$, then $\bar{\xi}_i(\varphi) = (1 - o_i(\varphi))\bar{\xi}_i(\varphi) + o_i(\varphi)\rho(\bar{\xi}_i(\varphi))$, which means that there are no saturation in information transmission.

And $\rho(\bar{\xi}_i) = [\rho_1(\bar{\xi}_{i1}) \quad \rho_2(\bar{\xi}_{i2}) \quad \cdots \quad \rho_n(\bar{\xi}_{in})]^T$ is the saturation function, and $\rho(\bar{\xi}_{ij})(j = 1, 2, \dots, n)$ satisfies

$$\rho(\bar{\xi}_{ij}) = \begin{cases} \zeta_j, & \bar{\xi}_{ij} \geq \zeta_j, \\ \bar{\xi}_{ij}(\varphi), & -\zeta_j < \bar{\xi}_{ij}(\varphi) < \zeta_j, \\ -\zeta_j, & -\bar{\xi}_{ij}(\varphi) \leq -\zeta_j, \end{cases} \quad j = 1, 2, \dots, n,$$

Then, similar to Reference 33, the saturation signal $\rho(\bar{\xi}_i(\varphi))$ can be obtained as,

$$\rho(\bar{\xi}_i(\varphi)) = \chi_i(\varphi) + \bar{\xi}_i(\varphi), \quad (8)$$

where $\chi(\varphi)$ is a non-linear function satisfying the following condition with $0 < \nu < 1$,

$$\chi_i^T(\varphi)\chi_i(\varphi) \leq \nu \bar{\xi}_i^T(\varphi)\bar{\xi}_i(\varphi).$$

Combining (7) and (8), one gets

$$\begin{aligned}\xi_i^{\text{re}}(\varphi) &= (1 - o_i(\varphi))\bar{\xi}_i(\varphi) + o_i(\varphi)(\chi_i(\varphi) + \bar{\xi}_i(\varphi)) \\ &= \bar{\xi}_i(\varphi) + o_i(\varphi)\chi_i(\varphi).\end{aligned}\quad (9)$$

The deception attacks may lead to the reconstruction of transmitted data, making the synchronization error system unstable. The adversaries insert malicious attack signals to modify the actual system states in a random way. In brief, the deception attack model is as follows:

$$\xi_1(\varphi) = (1 - \lambda_i(\varphi))f(\xi(\varphi - d_i(\varphi))) + \lambda_i(\varphi)\bar{\xi}_i(\varphi), \quad (10)$$

where $f(\cdot)$ is a deception attack signal, which satisfies Assumption 1. $\lambda_i(\varphi)$ is stochastic random variable and governs by the Bernoulli distribution, it satisfies

$$\mathbb{E}\{\lambda(\varphi)\} = \text{Prob}\{\lambda(\varphi) = 1\} = \bar{\lambda}, \quad \mathbb{E}\{(\lambda(\varphi) - \bar{\lambda})\} = \text{Prob}\{\lambda(\varphi) = 0\} = \theta_2^2.$$

Remark 3. When deception attacks occur, they can affect the system's performance. Particularly, if $\lambda(\varphi) = 1$, then (10) can be written as $\xi_1(\varphi) = \bar{\xi}_i(\varphi)$, which indicates deception attack is not occur, so the signals are transmitted successfully. when $\lambda(\varphi) = 0$, then (10) can be written as $\xi_1(\varphi) = f(\xi(\varphi - d_i(\varphi)))$, which indicates deception attack occur, so that malicious signals are transmitted successfully.

Assumption 1 (46). The non-linear function $\mathfrak{h}(\xi(\varphi))$ and $f(\xi(\varphi))$ describing the nonlinear dynamics of the system and deception attack signal are satisfies the following conditions, respectively.

$$\begin{aligned}\|\mathfrak{h}(\xi(\varphi))\|_2 &\leq \|\mathcal{R}_1\xi(\varphi)\|_2, \\ \|f(\xi(\varphi))\|_2 &\leq \|\mathcal{R}_2\xi(\varphi)\|_2.\end{aligned}$$

where \mathcal{R}_1 and \mathcal{R}_2 are known constant matrices.

We will consider that replay attacks occur at random in this study, with the purpose of misleading the controller. The attackers are considered to be able to collect and record a limited amount of networked transmitted signals. When replay attack occurs, a replay attack will be selected from the recorded data and it will sent through network. The stochastic random variable $\mu_i(\varphi)$ satisfying the Bernoulli distribution, which represent the occurrence of replay attacks is introduced. The signal sent through the network can then be reconstructed as

$$\xi_2(\varphi) = (1 - \mu_i(\varphi))\xi_r(\varphi) + \mu_i(\varphi)\xi_1(\varphi), \quad (11)$$

where $\xi_r(\varphi) = \bar{\xi}(\varphi - r_i(\varphi))$ is replay signal, and $r_i(\varphi)$ represents that the replayed data are the data transmitted in previous $r_i(\varphi)$ seconds. $\mathbb{E}\{\mu(\varphi)\} = \bar{\mu}$, $\mathbb{E}\{(\mu(\varphi) - \bar{\mu})\} = \theta_3^2$. The replay attack often considered to happen at a certain time interval. Then, $0 < r(\varphi) \leq r_N$, where $r(\varphi)$ has an upper bound r_N .

Assumption 2 (48). The transmission data are assumed to be stored from instant φ_0 to current instant φ , and then the data of an arbitrary instant from the sequence are selected for replay.

As discussed in Reference 40, DoS attacks contain the sleeping period and the active period. In this article, we assume that DoS attacks are detectable and denote DoS attacks as:

$$\xi_3(\varphi) = \begin{cases} 0, & \varphi \in [b_n, b_n + l_n) \\ \xi_2(\varphi), & \varphi \in [b_n + l_n, b_{n+1}), \end{cases} \quad (12)$$

where $\mathbf{L}_n \triangleq [b_n + l_n, b_{n+1})$ and $\mathbf{B}_n \triangleq [b_n, b_n + l_n)$ are represents the active and sleeping period of the n th DoS attack, respectively. Its satisfies $0 < h < l_n < \infty$ and $0 < l_n < b_{n+1} - b_n < \infty$.

Assumption 3 (40). Let b_{\max} and \mathbf{I}_n indicates the unified upper bound and lower bound of the active and sleep period, respectively.

$$\begin{cases} l_{\min} & \leq \inf\{l_n\} \\ b_{\max} & \geq \sup\{b_n - b_{n-1} - l_{n-1}\}. \end{cases} \quad (13)$$

Assumption 4 (40). The number of DoS sleep/active transitions in the interval $[\wp_0, \wp_1)$ is defined as $n(\wp_0, \wp_1)$. There exist $\epsilon \geq 0$ and $\mathfrak{F} \geq 0$ that should satisfy

$$n(\wp_0, \wp_1) \leq \epsilon + \frac{\wp_1 - \wp_0}{\mathfrak{F}}. \quad (14)$$

Remark 4. In practical engineering, communication networks are vulnerable to malicious network attacks, which is one of the important components affecting network security. Many synchronization controls for CNs with different types attacks are discussed in References 13,38, and 48. Due to the lack of research on the synchronization of CNs under cyber-attacks, the dissemination of related work is still very few.^{27,46} However, no research into DoS, deception, and reply hybrid cyber-attacks at the same time in a synchronization complex network has been conducted. In contrast to the previous debates, in this article, communication networks are considered to be vulnerable to hybrid cyber-attacks, such as replay, deception, and DoS attacks. Therefore, it is further presumed that the deception attack and replay attacks are secured by Bernoulli distributions, $\lambda(\wp)$ and $\mu(\wp)$, respectively.

Then Combining (9)–(12), we get,

$$\hat{\xi}(\wp) = \begin{cases} [(1 - \mu_i(\wp))\xi(\wp - r_i(\wp)) + (1 - \mu_i(\wp))\delta_{r_i}(\wp) + \mu_i(\wp)(1 - \lambda_i(\wp))f(\xi(\wp - d_i(\wp))) + \mu_i(\wp)\lambda_i(\wp) \\ \delta_i(\wp) + \mu_i(\wp)\lambda_i(\wp)\xi(\wp - \phi_i(\wp)) + \mu_i(\wp)\lambda_i(\wp)o_i(\wp)\chi_i(\wp)], & \wp \in \mathfrak{R}_k \cap \mathbf{B}_n \\ 0, & \wp \in \mathbf{L}_n. \end{cases} \quad (15)$$

We consider the control input $u_i(\wp)$ as

$$u_i(\wp) = K_i \hat{\xi}(\wp). \quad (16)$$

Combining (4), (15), and (16), we obtain the output synchronization error system as follows,

$$\dot{\xi}_i(\wp) = \begin{cases} \bar{C}_i \xi_i(\wp) + D_i \bar{h}(\xi_i(\wp)) + \alpha_i \sum_{j=1}^N g_{ij} \bar{\Lambda} \xi_j(\wp) + b_i D_i K_i [(1 - \mu_i(\wp))\xi(\wp - r_i(\wp)) + \mu_i(\wp)\lambda_i(\wp) \\ o_i(\wp)\chi_i(\wp) + \mu_i(\wp)(1 - \lambda_i(\wp))f(\xi(\wp - d_i(\wp))) + (1 - \mu_i(\wp))\delta_{r_i}(\wp) + \mu_i(\wp)\lambda_i(\wp)\delta_i(\wp) \\ + \mu(\wp)\lambda_i(\wp)\xi(\wp - \phi_i(\wp))], & \wp \in \mathfrak{R}_k \cap \mathbf{B}_n, \\ \bar{C}_i \xi_i(\wp) + D_i \bar{h}(\xi_i(\wp)) + \alpha_i \sum_{j=1}^N g_{ij} \bar{\Lambda} \xi_j(\wp), & \wp \in \mathbf{L}_n. \end{cases} \quad (17)$$

By using the Kronecker product, the error dynamical network (17) can be written as,

$$\dot{\xi}(\wp) = \begin{cases} \bar{C} \xi(\wp) + D \bar{h}(\xi(\wp)) + (G \otimes \alpha \bar{\Lambda}) \xi_j(\wp) + BDK[(1 - \mu(\wp))\xi(\wp - r_i(\wp)) + \mu(\wp)\lambda(\wp)o(\wp)\chi(\wp) \\ + \mu(\wp)\lambda_i(\wp)(1 - \lambda(\wp))f(\xi(\wp - d(\wp))) + (1 - \mu(\wp))\delta_r(\wp) + \mu(\wp)\lambda(\wp)\delta(\wp) \\ + \mu(\wp)\lambda(\wp)\xi(\wp - \phi(\wp))], & \wp \in \mathfrak{R}_k \cap \mathbf{B}_n, \\ \bar{C} \xi(\wp) + D \bar{h}(\xi(\wp)) + (G \otimes \alpha \bar{\Lambda}) \xi_j(\wp), & \wp \in \mathbf{L}_n, \end{cases} \quad (18)$$

where,

$$\begin{aligned} \bar{C} &= \text{diag}_{\mathbf{N}}\{\bar{C}_i\}, D = \text{diag}_{\mathbf{N}}\{D_i\}, K = \text{diag}_{\mathbf{N}}\{K_i\}, o(\wp) = \text{diag}_{\mathbf{N}}\{o_i(\wp)\} \otimes I, \lambda(\wp) = \text{diag}_{\mathbf{N}}\{\lambda_i(\wp)\} \otimes I, \\ \mu(\wp) &= \text{diag}_{\mathbf{N}}\{\mu_i(\wp)\} \otimes I, \alpha = \text{diag}_{\mathbf{N}}\{\alpha_i\}, \xi(\wp) = \text{col}_{\mathbf{N}}\{\xi_i(\wp)\}, \bar{h}(\xi(\wp)) = \text{col}_{\mathbf{N}}\{\bar{h}_i(\xi_i(\wp))\}, \chi(\wp) = \text{col}_{\mathbf{N}}\{\chi_i(\wp)\}, \bar{f}(\xi(\wp) - \\ d(\wp)) &= \text{col}_{\mathbf{N}}\{\bar{f}_i(\xi_i(\wp) - d_i(\wp))\}, \xi(\wp - \phi(\wp)) = \text{col}_{\mathbf{N}}\{\xi_i(\wp - \phi_i(\wp))\}, \delta_r(\wp) = \text{col}_{\mathbf{N}}\{\delta_{r_i}(\wp)\}. \end{aligned}$$

Lemma 1 (37). For a constant $\phi > 0$, if the function $\phi(\varrho)$ satisfies $0 < \phi(\varrho) \leq \phi_N$, there exist $\mathcal{V} > 0$ such that

$$-\int_{\varrho-\phi_N}^{\varrho} \dot{\xi}^T(r) \mathcal{V}_1 \dot{\xi}(\varrho) dr \leq \begin{bmatrix} \xi^T(\varrho) \\ \xi^T(\varrho - \phi(\varrho)) \\ \xi^T(\varrho - \phi_N) \end{bmatrix}^T \begin{bmatrix} -\mathcal{V}_1 & \mathcal{V}_1 & 0 \\ * & -2\mathcal{V}_1 & \mathcal{V}_1 \\ * & * & -\mathcal{V}_1 \end{bmatrix} \begin{bmatrix} \xi^T(\varrho) \\ \xi^T(\varrho - \phi(\varrho)) \\ \xi^T(\varrho - \phi_N) \end{bmatrix}.$$

Lemma 2 (47). For a given positive-definite matrices \mathcal{J}, \mathcal{L} and a scalar τ , the following inequality holds:

$$-\mathcal{J}\mathcal{L}^{-1}\mathcal{J} \leq -2\tau\mathcal{J} + \tau^2\mathcal{L}.$$

3 | MAIN RESULTS

Theorem 1. For the given positive scalars ν, κ, α , and $0 \leq \varepsilon \leq 1$. ϕ_N, d_N , and r_N denotes the upper bound of $\phi(\varrho), d(\varrho)$, and $r(\varrho)$, respectively. The random Bernoulli variables $\bar{o}, \bar{\lambda}, \bar{\mu} \in [0, 1]$ are states the occurrence of the saturation, deception attacks and replay attacks, respectively. The DoS attacks parameters are $\mathfrak{S}, \epsilon, b_{max}$ and l_{min} . The output dynamic synchronization error system (18) is asymptotically stable if there exist positive matrices $\mathcal{T}_i, \mathcal{U}_i, \mathcal{V}_i, (i = 1, 2, 3), (i = 1, 2.)$ with the proper dimension and event-triggered weighting matrix Θ such that the following conditions hold.

$$\Gamma_i \leq 0, \tag{19}$$

$$\frac{-2\aleph_1 l_{min} + 2\aleph_2 b_{max} + \ln(\rho_1 \rho_2) + 2(\aleph_1 + \aleph_2)h}{\mathfrak{S}} < 0, \tag{20}$$

$$\begin{cases} \mathcal{T}_1 \leq \rho_2 \mathcal{T}_2, \\ \mathcal{T}_2 \leq \rho_1 e^{2(\aleph_1 + \aleph_2)h} \mathcal{T}_1, \end{cases} \tag{21}$$

$$\begin{cases} \mathcal{U}_i \leq \rho_{3-i} \mathcal{U}_{(3-i)_j}, \\ \mathcal{V}_i \leq \rho_{3-i} \mathcal{V}_{(3-i)_j}. \end{cases} \tag{22}$$

And

$$\Gamma_1 = \begin{bmatrix} \Upsilon_{10 \times 10} & \Delta_0 & \Delta_{00} & \Delta_1 & \Delta_2 & \Delta_3 & \Delta_4 & \Delta_5 & \Delta_6 \\ * & -I^{-1} & 0 & 0 & 0 & 0 & 0 & 0 & 0 \\ * & * & -I^{-1} & 0 & 0 & 0 & 0 & 0 & 0 \\ * & * & * & \nabla_1 & 0 & 0 & 0 & 0 & 0 \\ * & * & * & * & \nabla_2 & 0 & 0 & 0 & 0 \\ * & * & * & * & * & \nabla_3 & 0 & 0 & 0 \\ * & * & * & * & * & * & \nabla_4 & 0 & 0 \\ * & * & * & * & * & * & * & -I & 0 \\ * & * & * & * & * & * & * & * & -I \end{bmatrix},$$

$$\Gamma_2 = \begin{bmatrix} Y'_{11} & Y'_{12} & Y'_{13} & Y'_{14} & 0 & 0 & 0 & 0 & 0 & 0 \\ * & Y'_{22} & 0 & 0 & Y'_{25} & 0 & 0 & Y'_{28} & 0 & 0 \\ * & * & Y'_{33} & 0 & 0 & 0 & 0 & 0 & Y'_{39} & 0 \\ * & * & * & Y'_{44} & 0 & 0 & 0 & 0 & 0 & Y'_{4,10} \\ * & * & * & * & Y'_{55} & 0 & 0 & 0 & 0 & 0 \\ * & * & * & * & * & Y'_{66} & 0 & 0 & 0 & 0 \\ * & * & * & * & * & * & Y'_{77} & 0 & 0 & 0 \\ * & * & ** & * & * & * & * & Y'_{88} & 0 & 0 \\ * & * & * & * & * & * & * & * & Y'_{99} & 0 \\ * & * & * & * & * & * & * & * & * & Y'_{10,10} \end{bmatrix},$$

where

$$\begin{aligned} Y_{11} &= \bar{C}\mathcal{T}_1 + \mathcal{T}_1\bar{T} + e^{-2\mathcal{N}_1\phi_N}\mathcal{U}_1 + e^{-2\mathcal{N}_1d_N}\mathcal{U}_2 + e^{-2\mathcal{N}_1r_N}\mathcal{U}_3 - \mathcal{V}_1 - \mathcal{V}_2 - \mathcal{V}_3 + \nu, \\ Y_{13} &= e^{-2\mathcal{N}_1d_N}\mathcal{V}_2, Y_{12} = \mathcal{T}\alpha(G \otimes \bar{\Lambda}) + \mathcal{T}BDK\bar{\lambda}\bar{\mu} + e^{-2\mathcal{N}_1\phi_N}\mathcal{V}_1, Y_{14} = \mathcal{T}BDK(1 - \bar{\mu}) \\ &\quad + e^{-2\mathcal{N}_1r_N}\mathcal{V}_3, Y_{15} = \mathcal{T}BDK\bar{\lambda}\bar{\mu}, Y_{16} = \mathcal{T}BDK(1 - \bar{\mu}), Y_{17} = \mathcal{T}BDK\bar{o}\bar{\lambda}\bar{\mu}, \\ Y_{22} &= -2e^{-2\mathcal{N}_1\phi_N}\mathcal{V}_1 + \nu(\Theta + 1), Y_{2,8} = e^{-2\mathcal{N}_1\phi_N}\mathcal{V}_1, Y_{33} = -2e^{-2\mathcal{N}_1d_N}\mathcal{V}_2, Y_{3,9} = e^{-2\mathcal{N}_1d_N}\mathcal{V}_2, \\ Y_{25} &= \nu, Y_{44} = -2e^{-2\mathcal{N}_1r_N}\mathcal{V}_3 + \nu\Theta, Y_{4,10} = e^{-2\mathcal{N}_1r_N}\mathcal{V}_3, Y_{55} = -\nu(\kappa\Theta + 1), Y_{66} = -\nu\kappa\Theta, Y_{77} = -I, \\ Y_{8,8} &= -e^{-2\mathcal{N}_1\phi_N}\mathcal{U}_1 - e^{-2\mathcal{N}_1\phi_N}\mathcal{V}_1, Y_{9,9} = -e^{-2\mathcal{N}_1d_N}(\mathcal{U}_2 - \mathcal{V}_2), Y_{10,10} = -e^{-2\mathcal{N}_1r_N}(\mathcal{U}_3 - \mathcal{V}_3), \\ Y'_{11} &= \bar{C}\mathcal{T}_2 + \mathcal{T}_2\bar{T} + e^{-2\mathcal{N}_2\phi_N}\mathcal{U}_2 + e^{-2\mathcal{N}_2d_N}\mathcal{U}_2 + e^{-2\mathcal{N}_2r_N}\mathcal{U}_3 - \mathcal{V}_2 - \mathcal{V}_2 - \mathcal{V}_3 + \nu, Y'_{13} = e^{2\mathcal{N}_2d_N}\mathcal{V}_2, \\ Y'_{12} &= \mathcal{T}_2\alpha(G \otimes \bar{\Lambda}) + \mathcal{T}_2BDK\bar{\lambda}\bar{\mu} + e^{2\mathcal{N}_2\phi_N}\mathcal{V}_2, Y'_{14} = e^{2\mathcal{N}_2r_N}\mathcal{V}_3, Y'_{15} = \mathcal{T}_2BDK\bar{\lambda}\bar{\mu}, \\ Y'_{22} &= -2e^{2\mathcal{N}_2\phi_N}\mathcal{V}_2 + \nu(\Theta + 1), Y_{2,8} = e^{2\mathcal{N}_2\phi_N}\mathcal{V}_2, Y'_{33} = -2e^{2\mathcal{N}_2d_N}\mathcal{V}_2, Y_{3,9} = e^{2\mathcal{N}_2d_N}\mathcal{V}_2, \\ Y'_{25} &= \nu, Y_{44} = -2e^{2\mathcal{N}_2r_N}\mathcal{V}_3 + \nu\Theta, Y_{4,10} = e^{2\mathcal{N}_2r_N}\mathcal{V}_3, Y'_{55} = -\nu(\kappa\Theta + 1), Y'_{66} = -\nu\kappa\Theta, Y_{77} = -I, \\ Y'_{8,8} &= -e^{2\mathcal{N}_2\phi_N}\mathcal{U}_2 - e^{-2\mathcal{N}_2\phi_N}\mathcal{V}_2, Y'_{9,9} = -e^{2\mathcal{N}_2d_N}(\mathcal{U}_2 - \mathcal{V}_2), Y'_{10,10} = -e^{2\mathcal{N}_2r_N}(\mathcal{U}_3 - \mathcal{V}_3), \\ \Delta_0 &= [0 \quad \mathcal{T}_1D \quad 0_{10 \times 10}], \Delta_{00} = [\mathcal{T}_1BDK(1 - \bar{\lambda})\bar{\mu} \quad 0_{11 \times 11}], \\ \Delta_1 &= \{\mathcal{O}_1 \quad \mathcal{O}_2 \quad \mathcal{P}_1 \quad \mathcal{P}_2 \quad \mathcal{P}_3 \quad \mathcal{P}_4 \quad \mathcal{P}_5 \quad \mathcal{P}_6\}, \Delta_2 = \{\mathcal{Q}_1 \quad \mathcal{Q}_2 \quad \mathcal{Q}_3 \quad \mathcal{Q}_4 \quad \mathcal{Q}_5 \quad \mathcal{Q}_6\}, \\ \Delta_3 &= \{\mathcal{R}_1 \quad \mathcal{R}_2 \quad \mathcal{R}_3 \quad \mathcal{R}_4 \quad \mathcal{R}_5 \quad \mathcal{R}_6\}, \Delta_4 = \{\mathcal{S}_1 \quad \mathcal{S}_2 \quad \mathcal{S}_3 \quad \mathcal{S}_4 \quad \mathcal{S}_5 \quad \mathcal{S}_6\}, \Delta_5 = [0_{10 \times 10} \quad \mathcal{R}_1 \quad 0] \\ \nabla_1 &= \text{diag}\{-\mathcal{T}_1, -\mathcal{T}_1, -\mathcal{T}_1\mathcal{V}_1\mathcal{T}_1, -\mathcal{T}_1\mathcal{V}_2\mathcal{T}_1, -\mathcal{T}_1\mathcal{V}_3\mathcal{T}_1, -\mathcal{T}_1\mathcal{V}_1\mathcal{T}_1, -\mathcal{T}_1\mathcal{V}_2\mathcal{T}_1 - \mathcal{T}_1\mathcal{V}_3\mathcal{T}_1\}, \\ \nabla_2 &= \text{diag}\{-\mathcal{T}_1\mathcal{V}_1\mathcal{T}_1, -\mathcal{T}_1\mathcal{V}_2\mathcal{T}_1, -\mathcal{T}_1\mathcal{V}_3\mathcal{T}_1, -\mathcal{T}_1\mathcal{V}_1\mathcal{T}_1, -\mathcal{T}_1\mathcal{V}_2\mathcal{T}_1, -\mathcal{T}_1\mathcal{V}_3\mathcal{T}_1\}, \Delta_6 = [0_{11 \times 11} \quad \mathcal{R}_2], \\ \nabla_3 &= \text{diag}\{-\mathcal{T}_1\mathcal{V}_1\mathcal{T}_1, -\mathcal{T}_1\mathcal{V}_2\mathcal{T}_1, -\mathcal{T}_1\mathcal{V}_3\mathcal{T}_1, -\mathcal{T}_1\mathcal{V}_1\mathcal{T}_1, -\mathcal{T}_1\mathcal{V}_2\mathcal{T}_1, -\mathcal{T}_1\mathcal{V}_3\mathcal{T}_1\}, \mathcal{O}_1 = \{\mathcal{T}_1\mathcal{R}_1 \quad 0_{11 \times 11}\} \\ \nabla_4 &= \text{diag}\{-\mathcal{T}_1\mathcal{V}_1\mathcal{T}_1, -\mathcal{T}_1\mathcal{V}_2\mathcal{T}_1, -\mathcal{T}_1\mathcal{V}_3\mathcal{T}_1, -\mathcal{T}_1\mathcal{V}_1\mathcal{T}_1, -\mathcal{T}_1\mathcal{V}_2\mathcal{T}_1, -\mathcal{T}_1\mathcal{V}_3\mathcal{T}_1\}, \mathcal{O}_2 = \{\mathcal{T}_1\mathcal{R}_2 \quad 0_{11 \times 11}\}, \\ \mathbb{P}_j &= \{\tau_j\bar{C}\mathcal{T}_1 + \alpha(G \otimes \bar{\Lambda})\tau_j\mathcal{T}_1 \quad \bar{o}\bar{\lambda}\bar{\mu}\tau_j\mathcal{T}_1BDK \quad 0 \quad (1 - \bar{\mu})\tau_j\mathcal{T}_1BDK \quad \bar{\mu}\bar{\lambda}\tau_j\mathcal{T}_1BDK \\ &\quad \times \mathcal{T}_1BDK \quad (1 - \bar{\mu})\tau_j\mathcal{T}_1BDK \quad \bar{o}\bar{\lambda}\bar{\mu}\tau_j\mathcal{T}_1BDK \quad (1 - \bar{\lambda})\bar{\mu}\tau_j\mathcal{T}_1BDK \quad 0_{2 \times 2} \quad \tau_j\mathcal{T}_1D \quad 0\}, \\ \mathbb{P}_k &= \{0_{6 \times 6} \quad \theta_1\tau_j\bar{\lambda}\bar{\mu}\phi_N\mathcal{T}_1BDK \quad 0_{5 \times 5}\}, \mathcal{Q}_j = \{0_{1 \times 1} \quad \theta_2\bar{\mu}\tau_j\mathcal{T}_1BDK \quad 0_{2 \times 2} \quad \theta_2\bar{\mu}\tau_j\mathcal{T}_1BDK \\ &\quad 0 \quad \theta_2\bar{o}\bar{\mu}\tau_j\mathcal{T}_1BDK \quad 0_{4 \times 4} \quad -\theta_2\bar{\mu}\tau_j\mathcal{T}_1BDK\}, \mathcal{Q}_k = \{0 \quad \theta_3\bar{\lambda}\tau_j\mathcal{T}_1BDK \quad 0 \quad -\theta_3\tau_j\mathcal{T}_1BDK \\ &\quad \theta_3\bar{\lambda}\tau_j\mathcal{T}_1BDK \quad -\theta_3\tau_j\mathcal{T}_1BDK \quad \theta_3\bar{o}\bar{\lambda}\tau_j\mathcal{T}_1BDK \quad 0_{4 \times 4} \quad \theta_3(1 - \bar{\lambda})\tau_j\mathcal{T}_1BDK\}, \mathbb{R}_j = \{0_{6 \times 6} \\ &\quad \theta_1\theta_2\bar{\mu}\tau_j\mathcal{T}_1BDK \quad 0_{5 \times 5}\}, \mathcal{S}_j = \{0_{6 \times 6} \quad \theta_1\theta_3\tau_j\mathcal{T}_1BDK \quad 0_{5 \times 5}\}, \mathcal{S}_k = \{0_{6 \times 6} \quad \theta_1\theta_2\theta_3\tau_j\mathcal{T}_1BDK \quad 0_{5 \times 5}\} \\ \mathbb{R}_k &= \{0 \quad \theta_2\theta_3\tau_j\mathcal{T}_1BDK \quad 0_{2 \times 2} \quad \theta_2\theta_3\tau_j\mathcal{T}_1BDK \quad 0 \quad \theta_2\theta_3\bar{o}\tau_j\mathcal{T}_1BDK \quad 0_{4 \times 4} \quad -\theta_2\theta_3\tau_j\mathcal{T}_1BDK\}, \end{aligned}$$

and $\tau_1 = \tau_4 = \phi_N, \tau_2 = \tau_5 = d_N, \tau_3 = \tau_6 = r_N, (1 \leq j \leq 3), (4 \leq k \leq 6)$.

Proof. We consider the Lyapunov functional candidate as,

$$V(\varphi) = \begin{cases} V_{1_j}(\varphi), & \varphi \in \mathfrak{R} \cap \mathbf{B}_n, \\ V_{2_j}(\varphi), & \varphi \in \mathbf{L}_n, \end{cases} \tag{23}$$

where,

$$\begin{aligned} V_{i_1}(\varphi) &= \xi^T(\varphi)\mathcal{T}_i\xi(\varphi), \\ V_{i_2}(\varphi) &= \int_{\varphi-\phi_N}^{\varphi} \mathfrak{D}_i\xi^T(r)\mathcal{U}_{i_1}\xi(r)dr + \int_{\varphi-d_N}^{\varphi} \mathfrak{D}_i\xi^T(r)\mathcal{U}_{i_2}\xi(r)dr + \int_{\varphi-r_N}^{\varphi} \mathfrak{D}_i\xi^T(r)\mathcal{U}_{i_3}\xi(r)dr, \\ V_{i_3}(\varphi) &= \phi_N \int_{\varphi-\xi_N}^{\varphi} \int_r^{\varphi} \mathfrak{D}_i\xi^T(r)\mathcal{V}_{i_1}\xi(r)drd\varphi + d_N \int_{\varphi-d_N}^{\varphi} \int_r^{\varphi} \mathfrak{D}_i\xi^T(r)\mathcal{V}_{i_2}\xi(r)drd\varphi \\ &\quad + r_N \int_{\varphi-r_N}^{\varphi} \int_r^{\varphi} \mathfrak{D}_i\xi^T(r)\mathcal{V}_{i_3}\xi(r)drd\varphi, \end{aligned}$$

where $\mathfrak{D}_i = e^{(-1)i2\mathfrak{N}_i(\varphi-r)}$.

When $i = 1$ then time derivative of the Lyapunov function $V_{1_j}(\varphi)$ and taking expectation on it, we get

$$\begin{aligned} \mathbb{E}\{\dot{V}_{1_1}(\varphi)\} &= 2\xi^T(\varphi)\mathcal{T}_1\dot{\xi}(\varphi) \\ &= 2\xi^T(\varphi)\mathcal{T}_1[\bar{C}\xi_i(\varphi) + D\bar{h}(\xi_i(\varphi)) + \alpha(G \otimes \bar{\Lambda})\xi_j(\varphi) + BDK[(1 - \mu(\varphi))\xi_r(\varphi) + \mu(\varphi)\lambda(\varphi) \\ &\quad \times o(\varphi)\chi(\varphi) + \mu(\varphi)(1 - \lambda(\varphi))f(\xi(\varphi - d(\varphi)))] + (1 - \mu(\varphi))\delta_r(\varphi) + \mu(\varphi)\lambda(\varphi)\delta(\varphi) \\ &\quad + \mu(\varphi)\lambda(\varphi)\xi(\varphi - \phi(\varphi))], \end{aligned} \tag{24}$$

$$\begin{aligned} \mathbb{E}\{\dot{V}_{1_2}(\varphi)\} &= \xi^T(\varphi)(\mathcal{U}_{1_1} + \mathcal{U}_{1_2} + \mathcal{U}_{1_3}) - \xi^T(\varphi)e^{-2\mathfrak{N}_1\phi_N}\phi_N\mathcal{U}_{1_1}\xi(\varphi) - \xi^T(\varphi)e^{-2\mathfrak{N}_1d_N}d_N\mathcal{U}_{1_2}\xi(\varphi) \\ &\quad - \xi^T(\varphi)e^{-2\mathfrak{N}_1r_N}r_N\mathcal{U}_{1_3}\xi(\varphi), \end{aligned} \tag{25}$$

$$\begin{aligned} \mathbb{E}\{\dot{V}_{1_3}(\varphi)\} &= \phi_N \int_{\varphi-\phi(\varphi)}^{\varphi} [\xi^T(\varphi)\mathcal{V}_{1_1}\xi(\varphi) - \xi^T(r)\mathcal{V}_{1_1}\xi(r)]dr + d_N \int_{\varphi-d(\varphi)}^{\varphi} [\xi^T(\varphi)\mathcal{V}_{1_2}\xi(\varphi) - \xi^T(r)\mathcal{V}_{1_2}\xi(r)]dr \\ &\quad + r_N \int_{\varphi-r(\varphi)}^{\varphi} [\xi^T(\varphi)\mathcal{V}_{1_3}\xi(\varphi) - \xi^T(r)\mathcal{V}_{1_3}\xi(r)]dr, \\ &= \mathbb{E}\{\phi_N^2\xi^T(\varphi)\mathcal{V}_{1_1}\xi(\varphi) + d_N^2\xi^T(\varphi)\mathcal{V}_{1_2}\xi(\varphi) + r_N^2\xi^T(\varphi)\mathcal{V}_{1_3}\xi(\varphi) - \int_{\varphi-\phi_N}^{\varphi} \xi^T(r)e^{-2\mathfrak{N}_1\phi_N}\mathcal{V}_{1_1}\xi(r)dr \\ &\quad - \int_{\varphi-d_N}^{\varphi} \xi^T(r)e^{-2\mathfrak{N}_1d_N}\mathcal{V}_{1_2}\xi(r)dr - \int_{\varphi-r_N}^{\varphi} \xi^T(r)e^{-2\mathfrak{N}_1r_N}\mathcal{V}_{1_3}\xi(r)dr\}, \end{aligned} \tag{26}$$

Applying Remark 3, we get

$$- \int_{\varphi-\phi_N}^{\varphi} \xi^T(r)e^{-2\mathfrak{N}_1\phi_N}\mathcal{V}_{1_1}\xi(\varphi)dr = e^{-2\mathfrak{N}_1\phi_N}\mathfrak{E}_1^T\Xi_1\mathfrak{E}_1, \tag{27}$$

$$- \int_{\varphi-d_N}^{\varphi} \xi^T(r)e^{-2\mathfrak{N}_1d_N}\mathcal{V}_{1_2}\xi(\varphi)dr = e^{-2\mathfrak{N}_1d_N}\mathfrak{E}_2^T\Xi_2\mathfrak{E}_2, \tag{28}$$

$$- \int_{\varphi-r_N}^{\varphi} \xi^T(r)e^{-2\mathfrak{N}_1r_N}\mathcal{V}_{1_3}\xi(\varphi)dr = e^{-2\mathfrak{N}_1r_N}\mathfrak{E}_3^T\Xi_3\mathfrak{E}_3, \tag{29}$$

where,

$$\mathfrak{E}_1^T = \begin{bmatrix} \xi^T(\varphi) \\ \xi^T(\varphi - \phi(\varphi)) \\ \xi^T(\varphi - \phi_N) \end{bmatrix}, \mathfrak{E}_2^T = \begin{bmatrix} \xi^T(\varphi) \\ \xi^T(\varphi - d(\varphi)) \\ \xi^T(\varphi - d_N) \end{bmatrix}, \mathfrak{E}_3^T = \begin{bmatrix} \xi^T(\varphi) \\ \xi^T(\varphi - r(\varphi)) \\ \xi^T(\varphi - r_N) \end{bmatrix},$$

$$\Xi_1 = \begin{bmatrix} -\mathcal{V}_1 & \mathcal{V}_1 & 0 \\ * & -2\mathcal{V}_1 & \mathcal{V}_1 \\ * & * & -\mathcal{V}_1 \end{bmatrix}, \Xi_2 = \begin{bmatrix} -\mathcal{V}_2 & \mathcal{V}_2 & 0 \\ * & -2\mathcal{V}_2 & \mathcal{V}_2 \\ * & * & -\mathcal{V}_2 \end{bmatrix}, \Xi_3 = \begin{bmatrix} -\mathcal{V}_3 & \mathcal{V}_3 & 0 \\ * & -2\mathcal{V}_3 & \mathcal{V}_3 \\ * & * & -\mathcal{V}_3 \end{bmatrix}.$$

Note that

$$\begin{aligned} \mathbb{E}\{\dot{\xi}^T(\varphi)\bar{\mathcal{V}}\dot{\xi}(\varphi)\} &= A\bar{\mathcal{V}}A + \theta_1^2 B_1 \bar{\mathcal{V}}B_1 + \theta_2^2 B_2 \bar{\mathcal{V}}B_2 + \theta_3^2 B_3 \bar{\mathcal{V}}B_3 + \theta_1^2 \theta_2^2 \mathcal{O}_1 \bar{\mathcal{V}}\mathcal{O}_1 + \theta_2^2 \theta_3^2 \mathcal{O}_2 \bar{\mathcal{V}}\mathcal{O}_2 \\ &\quad + \theta_1^2 \theta_3^2 \mathcal{O}_3 \bar{\mathcal{V}}\mathcal{O}_3 + \theta_1^2 \theta_2^2 \theta_3^2 S \bar{\mathcal{V}}S, \end{aligned} \tag{30}$$

where $A = \bar{C}\xi(\varphi) + D\bar{h}(\xi(\varphi)) + \alpha(G \otimes \lambda)\xi(\varphi) + BDK\{(1 - \bar{\mu})\xi(\varphi - r(\varphi)) + (1 - \bar{\mu})\delta(\varphi - r(\varphi)) + \bar{\lambda}\bar{\mu}\xi(\varphi - \phi(\varphi)) + \bar{\lambda}\bar{\mu}\delta_\varphi + (1 - \bar{\lambda})\bar{\mu}f(\xi(\varphi - d(\varphi))) + \bar{o}\bar{\lambda}\bar{\mu}\chi(\varphi)\}$, $B_1 = BDK\{\bar{\lambda}\bar{\mu}\chi(\varphi)\}$, $B_2 = BDK\{\bar{\mu}\xi(\varphi - \phi(\varphi)) + \bar{\mu}\delta(\varphi) - \bar{\mu}f(\xi(\varphi - d(\varphi))) + \bar{o}\bar{\mu}\chi(\varphi)\}$, $B_3 = BDK\{-\xi(\varphi - r(\varphi)) - \delta(\varphi - r(\varphi)) + \bar{\lambda}\xi(\varphi - \phi(\varphi)) + \bar{\lambda}\delta(\varphi) + (1 - \bar{\lambda})f(\xi(\varphi - d(\varphi))) + \bar{o}\bar{\lambda}\bar{\mu}\}$, $\mathcal{O}_1 = \bar{\mu}BDK\chi(\varphi)$, $\mathcal{O}_2 = BDK\{\xi(\varphi - \phi(\varphi)) + \delta(\varphi) - f(\xi(\varphi - d(\varphi))) + \bar{o}\chi(\varphi)\}$, $\mathcal{O}_3 = \bar{\lambda}BDK\chi(\varphi)$, $S = BDK\chi(\varphi)$ and $\bar{\mathcal{V}} = \phi^2\mathcal{V}_1 + d^2\mathcal{V}_2 + r^2\mathcal{V}_3$. ■

From the Assumption 1, we have

$$\mathfrak{h}^T(\xi(\varphi))\mathfrak{h}(\xi(\varphi)) - \xi^T(\varphi)\mathcal{R}_1^T\mathcal{T}\mathcal{R}_1\xi(\varphi) \geq 0, \tag{31}$$

$$f^T(\xi(\varphi - d(\varphi)))f(\xi(\varphi - d(\varphi)))\xi^T(\varphi - d(\varphi)) - \mathcal{R}_2^T\mathcal{T}\mathcal{R}_2\xi(\varphi - d(\varphi)) \geq 0, \tag{32}$$

The saturation signal satisfies

$$v\bar{\xi}_i^T(\varphi)\bar{\xi}_i(\varphi) - \chi_i^T(\varphi)\chi_i(\varphi) \geq 0. \tag{33}$$

From (6), the AETS written as,

$$\xi^T(\varphi - \phi(\varphi))v\Theta\xi(\varphi - \phi_N(\varphi)) - \delta^T(\varphi)k\nu\Theta\delta(\varphi) \geq 0.$$

Furthermore combining (33)–(42), we get

$$\begin{aligned} \mathbb{E}\{\dot{V}_1(\varphi)\} &= -2\mathfrak{N}_1\mathbb{E}\{V_1\}(\varphi) + 2\mathfrak{N}_1\xi^T(\varphi)\mathcal{T}\xi(\varphi) + \mathbb{E}\{\dot{V}_1(\varphi)\} + \mathbb{E}\{\dot{V}_2(\varphi)\} + \mathbb{E}\{\dot{V}_3(\varphi)\}, \\ \mathbb{E}\{\dot{V}_1(\varphi)\} &= -2\mathfrak{N}_1\mathbb{E}\{V_1\}(\varphi) + \Phi^T(\varphi)\Gamma_1\Phi(\varphi), \end{aligned} \tag{34}$$

where $\Phi^T(\varphi) = \{\xi^T(\varphi) \quad \xi^T(\varphi - \phi(\varphi)) \quad \xi^T(\varphi - d(\varphi)) \quad \xi^T(\varphi - r(\varphi)) \quad \delta^T(\varphi) \quad \delta_r^T(\varphi) \quad \chi^T(\varphi) \quad \xi^T(\varphi - \phi_N) \quad \xi^T(\varphi - d_M) \quad \xi^T(\varphi - r_N) \quad \bar{h}^T(\xi(\varphi)) \quad f^T(\xi(\varphi - d(\varphi)))\}$.

Therefore, if LMI (19) is satisfied for $i = 1$, we get $\mathbb{E}\{\dot{V}_1(\varphi)\} \leq -2\mathfrak{N}_1\mathbb{E}\{V_1(\varphi)\}$, $\varphi \in \mathfrak{R}_k \cap \mathbf{B}_n$.

From (19), when $i = 2$ then Processing $V_2(t)$ in the same way, one obtain

$$\mathbb{E}\dot{V}_2(\varphi) \leq 2\mathfrak{N}_2\mathbb{E}\{V_2(\varphi)\} + \Phi^T(\varphi)\Gamma_2\Phi(\varphi). \tag{35}$$

Therefore, if LMI (19) is satisfied for $i = 2$, we get $\mathbb{E}\{\dot{V}_2(\varphi)\} \leq 2\mathfrak{N}_2\mathbb{E}\{V_2(\varphi)\}$, $\varphi \in \mathbf{L}_n$.

According to the above inequalities, we have

$$\mathbb{E}\{V_1(\varphi)\} \leq -e^{-2\mathfrak{N}_1(\varphi - b_n)}\mathbb{E}V_1(b_n), \quad \varphi \in b_n, \tag{36}$$

$$\mathbb{E}\{V_2(\varphi)\} \leq -e^{-2\mathfrak{N}_2(\varphi - b_n - l_n)}\mathbb{E}V_1(b_n + l_n), \quad \varphi \in l_n. \tag{37}$$

From the Equation (23) and (24), we get the following

$$\mathbb{E}\{V_1(\mathcal{F})\} \leq \rho_2 \mathbb{E}\{V_2(b_n^-)\}, \tag{38}$$

$$\mathbb{E}\{V_2(\mathcal{F})\} \leq \rho_1 e^{2(\aleph_2 + \aleph_1)h} \mathbb{E}\{V_1((b_n + ln)^{-1})\}. \tag{39}$$

Define $\pi = 2(\aleph_1 + \aleph_2)$. Combining the above equation and $\mathcal{F} \in \mathbf{B}_n$, we get

$$\begin{aligned} \mathbb{E}\{V_1(\mathcal{F})\} &\leq e^{-2\aleph_1(\mathcal{F}-b_n)} \mathbb{E}\{V_1(b_n)\} \\ &\dots \\ &\leq e^{(\pi h + \ln(\rho_1 \rho_2) + 2\aleph_2 b_{\max} - 2\aleph_1 l_{\min})n(0, \mathcal{F})} \mathbb{E}\{V_1(0)\} \\ &\quad + \sum_{a=0}^{n(0, \mathcal{F})} e^{(2\aleph_2 b_{\max} - 2\aleph_1 l_{\min} + \ln(\rho_1 \rho_2))n(b_a, \mathcal{F})} e^{2\aleph_1 b_a} v(b_a). \end{aligned} \tag{40}$$

For $\mathcal{F} \in L_n$, we get

$$\begin{aligned} \mathbb{E}\{V_2(\mathcal{F})\} &\leq e^{2\aleph_2(\mathcal{F}-b_n-l_n)} \mathbb{E}\{V_2(b_n + l_n)\} \\ &\dots \\ &\leq \frac{1}{\rho_2} e^{(\pi h + \ln(\rho_1 \rho_2) + 2\aleph_2 b_{\max} - 2\aleph_1 l_{\min})n(0, \mathcal{F})} \mathbb{E}\{V_1(0)\} \\ &\quad + \frac{1}{\rho_2} \sum_{a=0}^{n(0, \mathcal{F})} e^{(2\aleph_2 b_{\max} - 2\aleph_1 l_{\min} + \ln(\rho_1 \rho_2))n(b_a, \mathcal{F})} e^{2\aleph_1 b_a} v(b_a). \end{aligned} \tag{41}$$

Let $\rho = \max\{1, \frac{1}{\rho_2}\}$, we get the following inequality

$$\begin{aligned} \mathbb{E}\{V_2(\mathcal{F})\} &\leq \rho e^{(\pi h + \ln(\rho_1 \rho_2) + 2\aleph_2 b_{\max} - 2\aleph_1 l_{\min})n(0, \mathcal{F})} \mathbb{E}\{V_1(0)\} \\ &\quad + \rho \sum_{a=0}^{n(0, \mathcal{F})} e^{(2\aleph_2 b_{\max} - 2\aleph_1 l_{\min} + \ln(\rho_1 \rho_2))n(b_a, \mathcal{F})} e^{2\aleph_1 b_a} v(b_a). \end{aligned} \tag{42}$$

Combining the Assumption 4, we obtain

$$\mathbb{E}\{V_2(\mathcal{F})\} \leq \rho \left[V_1(0)e_1^{\mathfrak{V}_1} + \sum_{p=0}^{n(0, \mathcal{F})} v(b_p)e^{\mathfrak{V}_2(b_p)} \right] e^{\mathfrak{V}_3}, \tag{43}$$

where,

$$\begin{aligned} \mathfrak{V}_1 &= \varepsilon [\ln(\rho_1 \rho_2) + 2(\aleph_1 + \aleph_2)h + 2\aleph_2 b_{\max} - 2\aleph_1 b_{\min}], \\ \mathfrak{V}_2 &= \left(\varepsilon - \frac{h_p}{\mathfrak{S}} \right) [\ln(\rho_1 \rho_2) + 2\aleph_2 b_{\max} - 2\aleph_1 l_{\min}]n(0, \mathcal{F}) + 2\aleph_1 b_a, \\ \mathfrak{V}_3 &= \frac{\mathcal{F}}{\mathfrak{S}} [\ln(\rho_1 \rho_2) + 2\aleph_2 b_{\max} - 2\aleph_1 l_{\min}]n(0, \mathcal{F}). \end{aligned}$$

From Equation (21), we have $\mathcal{F} \rightarrow \infty, e^{\mathfrak{V}_3(\mathcal{F})} \rightarrow 0$. Hence, $\mathbb{E}\{V(\mathcal{F})\} = 0$. Then the output synchronization error system (18) is asymptotically stable. This completes proof.

Theorem 2. For the given positive scalars ν, κ, α , and $0 \leq \varepsilon \leq 1$. ϕ_N, d_N and r_N denotes the upper bound of $\phi(\mathcal{F}), d(\mathcal{F})$ and $r(\mathcal{F})$, respectively. The random Bernoulli variables $\bar{\delta}, \bar{\lambda}, \bar{\mu} \in [0, 1]$ are states the occurrence of the saturation, deception attacks and replay attacks, respectively. The DoS attacks parameters are $\mathfrak{S}, \varepsilon, b_{\max}$ and l_{\min} . The controller gain $K = \mathcal{Y}\mathcal{T}_i^{-1}$, output dynamic synchronization error system (18) is asymptotically stable if there exist positive matrices $\tilde{\mathcal{T}}_i, \tilde{\mathcal{U}}_i, \tilde{\mathcal{V}}_i, (i = 1, 2, 3), (i = 1, 2.)$ with the proper dimension and event-triggered weighting

matrix Θ such that the following conditions hold.

$$\tilde{\Gamma}_1 = \begin{bmatrix} \tilde{Y}_{10 \times 10} & \tilde{\Delta}_0 & \tilde{\Delta}_{00} & \tilde{\Delta}_1 & \tilde{\Delta}_2 & \tilde{\Delta}_3 & \tilde{\Delta}_4 & \tilde{\Delta}_5 & \tilde{\Delta}_6 \\ * & I - 2\mathcal{X} & 0 & 0 & 0 & 0 & 0 & 0 & 0 \\ * & * & I - 2\mathcal{X} & 0 & 0 & 0 & 0 & 0 & 0 \\ * & * & * & \tilde{V}_1 & 0 & 0 & 0 & 0 & 0 \\ * & * & * & * & \tilde{V}_2 & 0 & 0 & 0 & 0 \\ * & * & * & * & * & \tilde{V}_3 & 0 & 0 & 0 \\ * & * & * & * & * & * & \tilde{V}_4 & 0 & 0 \\ * & * & * & * & * & * & * & -I & 0 \\ * & * & * & * & * & * & * & * & -I \end{bmatrix} < 0, \quad (44)$$

$$\tilde{\Gamma}_2 = \begin{bmatrix} \tilde{Y}'_{11} & \tilde{Y}'_{12} & \tilde{Y}'_{13} & \tilde{Y}'_{14} & 0 & 0 & 0 & 0 & 0 & 0 \\ * & \tilde{Y}'_{22} & 0 & 0 & \tilde{Y}'_{25} & 0 & 0 & \tilde{Y}'_{28} & 0 & 0 \\ * & * & \tilde{Y}'_{33} & 0 & 0 & 0 & 0 & 0 & \tilde{Y}'_{39} & 0 \\ * & * & * & \tilde{Y}'_{44} & 0 & 0 & 0 & 0 & 0 & \tilde{Y}'_{4,10} \\ * & * & * & * & \tilde{Y}'_{55} & 0 & 0 & 0 & 0 & 0 \\ * & * & * & * & * & \tilde{Y}'_{66} & 0 & 0 & 0 & 0 \\ * & * & * & * & * & * & \tilde{Y}'_{77} & 0 & 0 & 0 \\ * & * & ** & * & * & * & * & \tilde{Y}'_{88} & 0 & 0 \\ * & * & * & * & * & * & * & * & \tilde{Y}'_{99} & 0 \\ * & * & * & * & * & * & * & * & * & \tilde{Y}'_{10,10} \end{bmatrix} < 0, \quad (45)$$

where

$$\begin{aligned} \tilde{Y}_{11} &= \bar{C}\mathcal{T}_1 + \mathcal{T}_1\bar{T} + e^{-2\mathfrak{N}_1\phi_N}\tilde{U}_1 + e^{-2\mathfrak{N}_1\phi_N}\tilde{U}_2 + e^{-2\mathfrak{N}_1\phi_N}\tilde{U}_3 - \tilde{V}_1 - \tilde{V}_2 - \tilde{V}_3 + \nu, \\ \tilde{Y}_{12} &= \mathcal{X}\alpha(G \otimes \bar{\Lambda}) + \bar{\mu}\bar{\lambda}\mathcal{Y}BD + e^{-2\mathfrak{N}_1\phi_N}\tilde{V}_1, \tilde{Y}_{13} = e^{-2\mathfrak{N}_1d_N}\tilde{V}_2, \tilde{Y}_{15} = \mathcal{Y}BD\bar{\lambda}\bar{\mu}, \\ \tilde{Y}_{14} &= e^{-2\mathfrak{N}_1r_N}\mathcal{Y}BD(1 - \bar{\mu}) + \tilde{V}_3, \tilde{Y}_{16} = \mathcal{Y}BD(1 - \bar{\mu}), \tilde{Y}_{22} = -2e^{-2\mathfrak{N}_1\phi_N}\tilde{V}_1 + v\tilde{\Theta}, \\ \tilde{Y}_{17} &= \mathcal{Y}BD\bar{\delta}\bar{\lambda}\bar{\mu}, \tilde{Y}_{2,8} = e^{-2\mathfrak{N}_1\phi_N}\tilde{V}_1, \tilde{Y}_{44} = -2e^{-2\mathfrak{N}_1d_N}\tilde{V}_2, \tilde{Y}_{3,9} = e^{-2\mathfrak{N}_1d_N}\tilde{V}_2, \\ \tilde{Y}_{44} &= -2e^{-2\mathfrak{N}_1r_N}\tilde{V}_3 + v\tilde{\Theta}, \tilde{Y}_{4,10} = e^{-2\mathfrak{N}_1r_N}\tilde{V}_3, \tilde{Y}_{55} = -v\kappa\tilde{\Theta}, \tilde{Y}_{66} = -v\kappa\tilde{\Theta}, \tilde{Y}_{77} = -I, \\ \tilde{Y}_{88} &= -e^{-2\mathfrak{N}_1r_N}\tilde{U}_1 - e^{-2\mathfrak{N}_1\phi_N}\tilde{V}_1, \tilde{Y}_{9,9} = -e^{-2\mathfrak{N}_1d_N}\tilde{U}_2 - e^{-2\mathfrak{N}_1d_N}\tilde{V}_2, \tilde{Y}_{10,10} = -e^{-2\mathfrak{N}_1r_N}\tilde{U}_3 \\ &\quad - e^{-2\mathfrak{N}_1r_N}\tilde{V}_3, \tilde{Y}'_{11} = \bar{C}\mathcal{T}_2 + \mathcal{T}_2\bar{T} + e^{-2\mathfrak{N}_2\phi_N}\tilde{U}_2 + e^{-2\mathfrak{N}_2\phi_N}\tilde{U}_2 + e^{-2\mathfrak{N}_2\phi_N}\tilde{U}_3 - \tilde{V}_2 - \tilde{V}_2 - \tilde{V}_3 + \nu, \\ \tilde{Y}'_{12} &= \mathcal{X}\alpha(G \otimes \bar{\Lambda}) + e^{-2\mathfrak{N}_2\phi_N}\tilde{V}_2, \tilde{Y}'_{22} = -2e^{-2\mathfrak{N}_2\phi_N}\tilde{V}_2 + v\tilde{\Theta}, \tilde{Y}'_{2,8} = e^{-2\mathfrak{N}_2\phi_N}\tilde{V}_2, \\ \tilde{Y}'_{33} &= -2e^{-2\mathfrak{N}_2d_N}\tilde{V}_2, \tilde{Y}'_{3,9} = e^{-2\mathfrak{N}_2d_N}\tilde{V}_2, \tilde{Y}'_{44} = -2e^{-2\mathfrak{N}_2r_N}\tilde{V}_3 + v\tilde{\Theta}, \tilde{Y}'_{4,10} = e^{-2\mathfrak{N}_2r_N}\tilde{V}_3, \\ \tilde{Y}'_{55} &= -v\kappa\tilde{\Theta}, \tilde{Y}'_{66} = -v\kappa\tilde{\Theta}, \tilde{Y}'_{77} = -I, \tilde{Y}'_{14} = \tilde{V}_1, \tilde{Y}'_{88} = -e^{-2\mathfrak{N}_2\phi_N}\tilde{U}_2 - e^{-2\mathfrak{N}_2\phi_N}\tilde{V}_2, \\ \tilde{Y}'_{9,9} &= -e^{-2\mathfrak{N}_2d_N}\tilde{U}_2 - e^{-2\mathfrak{N}_2d_N}\tilde{V}_2, \tilde{Y}'_{10,10} = -e^{-2\mathfrak{N}_2r_N}\tilde{U}_3 - e^{-2\mathfrak{N}_2r_N}\tilde{V}_3, \tilde{\Delta}_0 = [0 \quad \tilde{T}_1D \quad 0_{10 \times 10}], \\ \tilde{\Delta}_{00} &= [\mathcal{Y}BD(1 - \bar{\lambda})\bar{\mu} \quad 0_{11 \times 11}], \tilde{\Delta}_1 = \{\tilde{O}_1 \quad \tilde{O}_2 \quad \tilde{P}_1 \quad \tilde{P}_2 \quad \tilde{P}_3 \quad \tilde{P}_4 \quad \tilde{P}_5 \quad \tilde{P}_6\}, \\ \tilde{\Delta}_2 &= \{\tilde{Q}_1 \quad \tilde{Q}_2 \quad \tilde{Q}_3 \quad \tilde{Q}_4 \quad \tilde{Q}_5 \quad \tilde{Q}_6\}, \tilde{\Delta}_3 = \{\tilde{R}_1 \quad \tilde{R}_2 \quad \tilde{R}_3 \quad \tilde{R}_4 \quad \tilde{R}_5 \quad \tilde{R}_6\}, \tilde{\Delta}_5 = [0_{10 \times 10} \quad \mathcal{R}_1\mathcal{X} \quad 0], \\ \tilde{\Delta}_4 &= \{\tilde{S}_1 \quad \tilde{S}_2 \quad \tilde{S}_3 \quad \tilde{S}_4 \quad \tilde{S}_5 \quad \tilde{S}_6\}, \tilde{\Delta}_6 = [0_{11 \times 11} \quad \mathcal{R}_2\mathcal{X}], \tilde{V}_2 = \text{diag}\{F_1, F_2, F_3, F_1, F_2, F_3\}, \\ \tilde{V}_1 &= \text{diag}\{-\tilde{\mathcal{X}}, -\tilde{\mathcal{X}}, F_1, F_2, F_3, F_1, F_2, F_3\}, \tilde{V}_3 = \text{diag}\{F_1, F_2, F_3, F_1, F_2, F_3\}, \end{aligned}$$

$$\begin{aligned} \tilde{V}_4 &= \text{diag}\{F_1, F_2, F_3, F_1, F_2, F_3\}, F_1 = -2\varepsilon_1\mathcal{X} + \varepsilon_1^2\tilde{\mathcal{V}}_{1_1}, F_2 = -2\varepsilon_2\mathcal{X} + \varepsilon_2^2\tilde{\mathcal{V}}_{1_2}, \\ F_3 &= -2\varepsilon_3\mathcal{X} + \varepsilon_3^2\tilde{\mathcal{V}}_{1_3}, \tilde{\mathcal{O}}_1 = \{\mathcal{X}\mathcal{R}_{1_1} \quad 0_{3 \times 3} \quad 0_{3 \times 3} \quad 0_{5 \times 5}\}, \tilde{\mathcal{O}}_2 = \{\mathcal{X}\mathcal{R}_{1_2} \quad 0_{5 \times 5} \quad 0 \quad 0_{3 \times 3} \quad 0 \quad 0\}, \\ \tilde{\mathbb{P}}_j &= \{\tau_j\bar{C}\mathcal{X} + \alpha(G \otimes \bar{\Lambda})\tau_j\mathcal{X} \quad \bar{o}\bar{\lambda}\tau_j\mathcal{Y}BD \quad 0 \quad (1 - \bar{\mu})\tau_j\mathcal{Y}BD \quad \bar{\mu}\bar{\lambda}\tau_j \\ \mathcal{Y}BD \quad (1 - \bar{\lambda})\tau_j\mathcal{Y}BD \quad \bar{o}\bar{\lambda}\bar{\mu}\tau_j\mathcal{Y}BD \quad (1 - \bar{\lambda})\bar{\mu}\tau_j\mathcal{Y}BD \quad 0_{2 \times 2} \quad \tau_j\mathcal{X}D \quad 0\}, \\ \tilde{\mathbb{Q}}_j &= \{0 \quad \theta_2\bar{\mu}\tau_j\mathcal{Y}BD \quad 0_{2 \times 2} \quad \theta_2\bar{\mu}\tau_j\mathcal{Y}BD \quad 0 \quad \theta_2\bar{o}\bar{\mu}\tau_j\mathcal{Y}BD \quad 0_{4 \times 4} \quad -\theta_2\bar{\mu}\tau_j\mathcal{Y}BD\}, \\ \tilde{\mathbb{Q}}_k &= \{0 \quad \theta_3\bar{\lambda}\tau_j\mathcal{Y}BD \quad 0 \quad -\theta_3\tau_j\mathcal{Y}BD \quad \theta_3\bar{\lambda}\tau_j\mathcal{Y}BD \quad -\theta_3\tau_j\mathcal{Y}BD \quad \theta_3\bar{o}\bar{\lambda}\tau_j\mathcal{Y}BD \\ 0_{4 \times 4} \quad \theta_3(1 - \bar{\lambda})\tau_j\mathcal{Y}BD\}, \tilde{\mathbb{P}}_k &= \{0_{6 \times 6} \quad \theta_1\bar{\lambda}\tau_j\bar{\mu}\mathcal{Y}BD \quad 0_{5 \times 5}\}, \tilde{\mathbb{R}}_j = \{0_{6 \times 6} \quad \theta_1\theta_2\bar{\mu}\tau_j\mathcal{Y}BD \\ 0_{5 \times 5}\}, \tilde{\mathbb{R}}_k &= \{0 \quad \theta_2\theta_3\tau_j\mathcal{Y}BD \quad 0_{2 \times 2} \quad \theta_2\theta_3\tau_j\mathcal{Y}BD \quad 0 \quad \theta_2\theta_3\bar{o}\tau_j\mathcal{Y}BD \quad 0_{4 \times 4} \quad -\theta_2\theta_3\tau_j\mathcal{Y}BD\}, \\ \tilde{\mathbb{S}}_j &= \{0_{6 \times 6} \quad \theta_1\theta_3\tau_j\mathcal{Y}BD \quad 0_{5 \times 5}\}, \tilde{\mathbb{S}}_k = \{0_{6 \times 6} \quad \theta_1\theta_2\theta_3\tau_j\mathcal{Y}BD \quad 0_{5 \times 5}\}, \end{aligned}$$

and $a_1 = a_4 = \phi_N, a_2 = a_5 = d_N, a_3 = a_6 = r_N, (1 \leq j \leq 3), (4 \leq k \leq 6)$. The adaptive event-triggered controller gains are computed as $K = \mathcal{Y}\mathcal{T}_i^{-1}$.

Proof. Define $\mathcal{X} = \mathcal{T}_i^{-1}, K\mathcal{T}_i = \mathcal{Y}$. Then pre and post-multiply both sides of Γ by $\mathbf{a} = \text{diag}\{\mathcal{X}, \mathcal{X}, \dots, \mathcal{X}, I, I\}$ and its transpose, respectively.

From Remark 4, we get $-\mathcal{T}_i\mathcal{V}_i^{-1}\mathcal{T}_i \leq -2\varepsilon_i\mathcal{T}_i + \varepsilon_i^2\mathcal{V}_i$ and $-\mathcal{X}I^{-1}\mathcal{X} \leq I - 2\mathcal{X}$, where $i = \{1, 2, 3\}$.

Denote that $\tilde{\mathcal{T}}_i = \mathcal{X}^T\mathcal{T}_i\mathcal{X}, \tilde{\mathcal{U}}_i = \mathcal{X}^T\mathcal{U}_i\mathcal{X}, \tilde{\mathcal{V}}_i = \mathcal{X}^T\mathcal{V}_i\mathcal{X}$, and applying the Schur complement, then $\tilde{\Gamma}_i$ can be obtained. This completes the proof. ■

4 | NUMERICAL EXAMPLES

Two numerical examples are given in this section to illustrate the efficacy of the suggested method.

Example 1. Consider output synchronization error system (27) for complex network under hybrid cyber-attacks with the following parameters:

$$\begin{aligned} \dot{\xi}(\varphi) &= \begin{cases} \bar{C}\xi(\varphi) + D\bar{\mathfrak{h}}(\xi(\varphi)) + (G \otimes \alpha\bar{\Lambda})\xi_j(\varphi) + BDK[(1 - \mu(\varphi))\xi(\varphi - r_i(\varphi)) + \mu(\varphi)\lambda(\varphi)o(\varphi)\chi(\varphi) \\ + \mu(\varphi)\lambda_i(\varphi)(1 - \lambda(\varphi))f(\xi(\varphi - d(\varphi))) + (1 - \mu(\varphi))\delta_r(\varphi) + \mu(\varphi)\lambda(\varphi)\delta(\varphi) \\ + \mu(\varphi)\lambda(\varphi)\xi(\varphi - \phi(\varphi))], & \varphi \in \mathfrak{R}_k \cap \mathbf{B}_n, \\ \bar{C}\xi(\varphi) + D\bar{\mathfrak{h}}(\xi(\varphi)) + (G \otimes \alpha\bar{\Lambda})\xi_j(\varphi), & \varphi \in \mathbf{L}_n, \end{cases} \quad (46) \\ C_1 &= \begin{bmatrix} 1 & 0.5 \\ 0.3 & 1.2 \end{bmatrix}, C_2 = \begin{bmatrix} 0.5 & 0.4 \\ 0.4 & 0.9 \end{bmatrix}, C_3 = \begin{bmatrix} 1.2 & 0.2 \\ 0.5 & 1.4 \end{bmatrix}, D_1 = \begin{bmatrix} 0.3 & 0 \\ 0 & 0.2 \end{bmatrix}, \\ D_2 &= \begin{bmatrix} 0.12 & 0 \\ 0 & 0.13 \end{bmatrix}, D_3 = \begin{bmatrix} 0.5 & 0 \\ 0 & 0.2 \end{bmatrix}, \mathcal{R}_1 = \begin{bmatrix} 3.3 & 0 \\ 0 & 3.4 \end{bmatrix}, \mathcal{R}_2 = \begin{bmatrix} 3.2 & 0 \\ 0 & 3.3 \end{bmatrix}, \\ B &= \begin{bmatrix} 0.01 & 0.1 \\ 0.1 & 0.01 \end{bmatrix}, I = \begin{bmatrix} 1 & 0 \\ 0 & 1 \end{bmatrix}. \end{aligned}$$

Let us assume the saturation signal is

$$\rho(\bar{\xi}_i) = \begin{cases} 0.08, & \bar{\xi}_j, \\ \bar{\xi}_j, & -0.08 < \bar{\xi}_j < 0.08, \\ -0.08, & -\bar{\xi}_j \leq -0.05. \end{cases}$$

We choose the non-linear function $\mathfrak{h} = [0.24 \tanh(\xi_{i1}(\varphi)) \quad 0.18 \tanh(\xi_{i2}(\varphi))]^T$ and deception attacks function $f(\xi(\varphi - d(\varphi))) = [-0.08 \tanh(\xi_2(\varphi)) \quad -0.8 \tanh(\xi_1(\varphi))]^T$, respectively.

The inner coupling matrix $\Lambda = \text{diag}\{0.8, 0.8\}$. The outer coupling matrix is

$$G = \begin{bmatrix} -2 & 1 & 1 \\ 1 & -2 & 1 \\ 1 & 1 & -2 \end{bmatrix}. \quad (47)$$

$$\Theta_1 = \begin{bmatrix} 4.8262 & -0.0158 \\ -0.0158 & 4.8063 \end{bmatrix}, \Theta_2 = \begin{bmatrix} 13.9872 & -0.4045 \\ -0.4045 & 13.1212 \end{bmatrix}, \Theta_3 = \begin{bmatrix} 4.0444 & 0.0643 \\ 0.0643 & 4.8427 \end{bmatrix},$$

$$K_1 = \begin{bmatrix} 7.5749 & 0.4609 \\ 0.4655 & 7.9912 \end{bmatrix}, K_2 = \begin{bmatrix} 7.5496 & 0.4415 \\ 0.4398 & 8.1984 \end{bmatrix}, K_3 = \begin{bmatrix} 8.0211 & 0.4629 \\ 0.4877 & 8.0992 \end{bmatrix}.$$

Let $\varepsilon_{i1} = 5, \varepsilon_{i2} = 5, \varepsilon_{i3} = 5, v_i = 0.9, \kappa_i = 2, \phi_N = 0.2, d_N = 0.5, r_N = 0.6, \nu = 4, \varepsilon_i = 3, (i = 1, 2, 3)$ and $\alpha_1(\varphi) = 0.4, \alpha_2(\varphi) = 0.65, \alpha_3(\varphi) = 0.39, \mathfrak{N}_1 = 0.4, \mathfrak{N}_2 = 0.2, \rho_1 = 0.08, \rho_2 = 0.9, \mathfrak{F} = 2.5, b_{\max} = 1.3,$ and $l_{\min} = 0.65$. The random Bernoulli variable choose $\bar{\delta} = 0.2, \bar{\lambda} = 0.7, \bar{\mu} = 0.5$ means that the synchronization error system are subjected to saturation, deception and replay attacks, concretely, the occurring probability. The following solutions are achieved by solving LMI in Theorem 2.

By using the MATLAB, the state trajectory of the synchronization error signal under hybrid cyber attacks with control and without control is shown in Figure 2 and 3 respectively. From these two figures, if there is no control input, the synchronization error signal's trajectory is divergent to origin under hybrid cyber attack otherwise convergent to origin. Figure 4 illustrates control input of the synchronization error signal for CNs with three different nodes. Figure 5–7 describes the release time instants and intervals under AETS for node 1–3, respectively. Figures 8 and 9 describes the saturation signal with and without control respectively.

Whenever the system only has deception attacks, the random Bernoulli variable $\lambda(\varphi)$, which denotes the occurrence of deception attacks is fix to $\bar{\lambda} = 0.7$. Figure 10 displays the state response of synchronization for CNs against deception attacks. The random variable $\bar{\lambda}$ represents the deception attacks, $\bar{\lambda} = 0.7$ are depicted in Figure 11. The release instants and intervals are shown in Figure 12.

Whenever the system only has replay attacks, the random Bernoulli variable $\mu(\varphi)$, which denotes the occurrence of deception attacks is fix to $\bar{\mu} = 0.5$. The state response of synchronization for CNs against replay attacks is shown in Figure 13. The random variable $\bar{\mu}$ represents the replay attacks, $\bar{\mu} = 0.5$ are depicted in Figure 14. The release instants and intervals are shown in Figure 15.

Whenever the system only has DoS attacks, DoS attacks parameters taken as $\mathfrak{F} = 2.5, \mathfrak{N}_1 = 0.4, \mathfrak{N}_2 = 0.2, \rho_1 = 0.08, \rho_2 = 0.9, b_{\max} = 1.3, l_{\min} = 0.65$. When the state response of synchronization for CNs against aperiodic DoS attacks

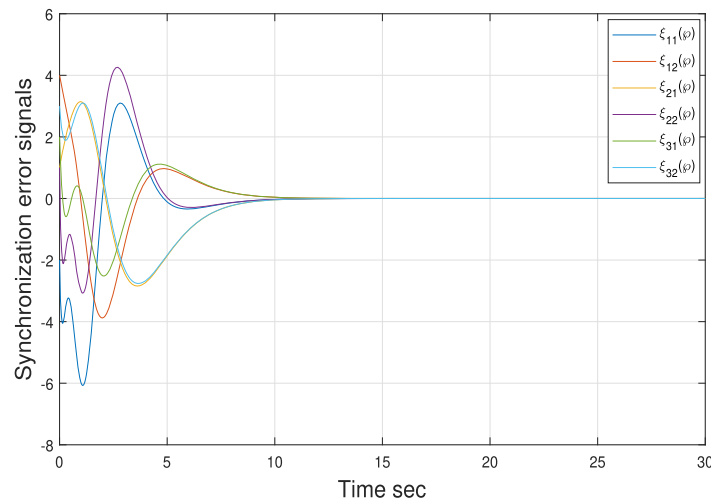


FIGURE 2 Synchronization errors with hybrid cyber-attacks under control.

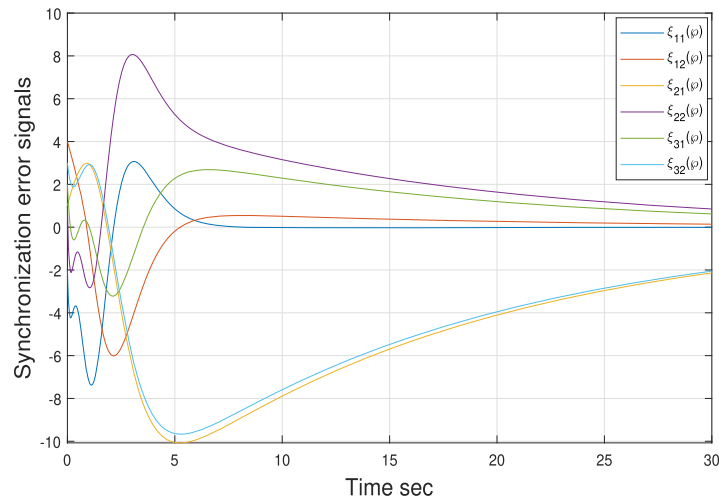


FIGURE 3 Synchronization errors with hybrid cyber-attacks without control.

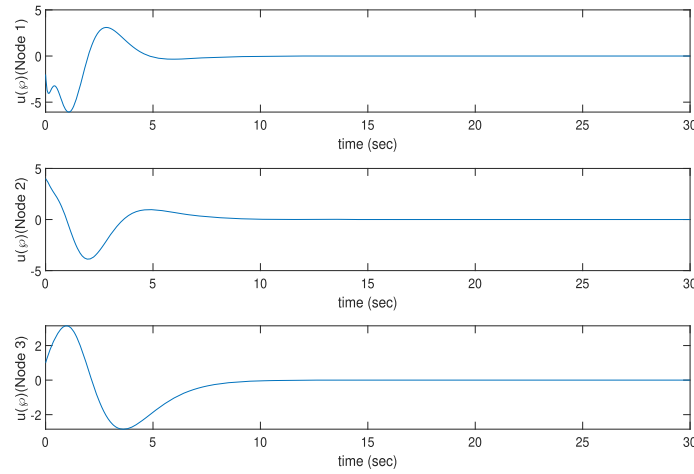


FIGURE 4 Control input $u(\varphi)$.

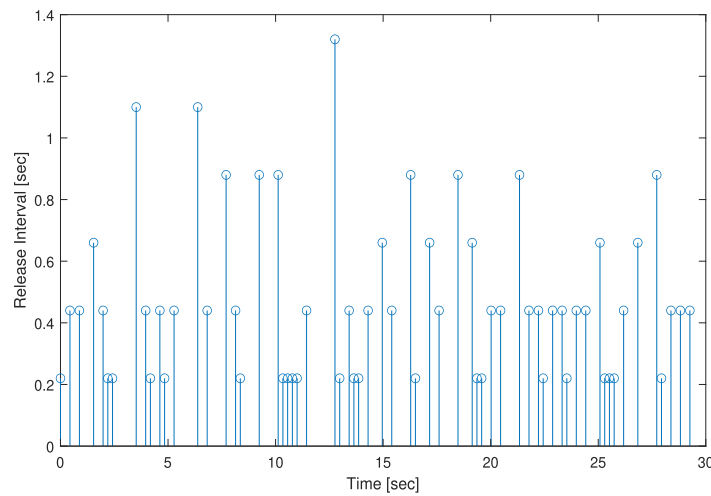


FIGURE 5 Release instants and intervals under AETS for node 1.

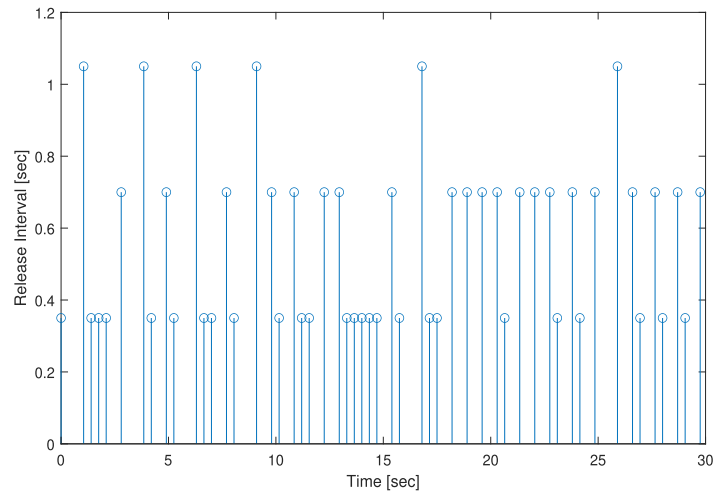


FIGURE 6 Release instants and intervals under AETS for node 2.

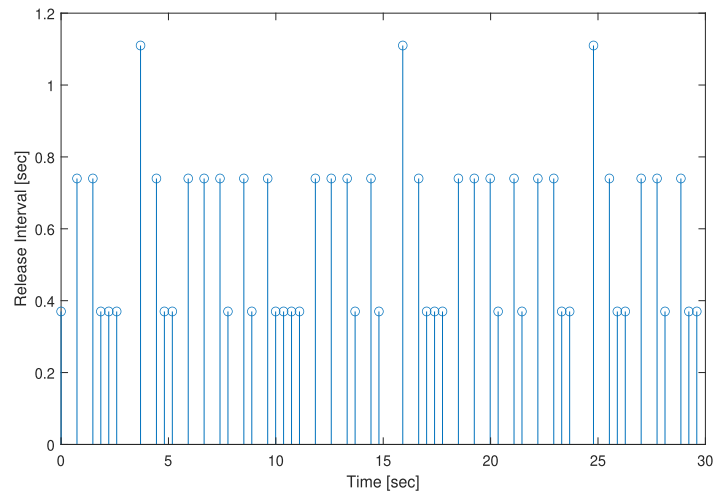


FIGURE 7 Release instants and intervals under AETS for node 3.

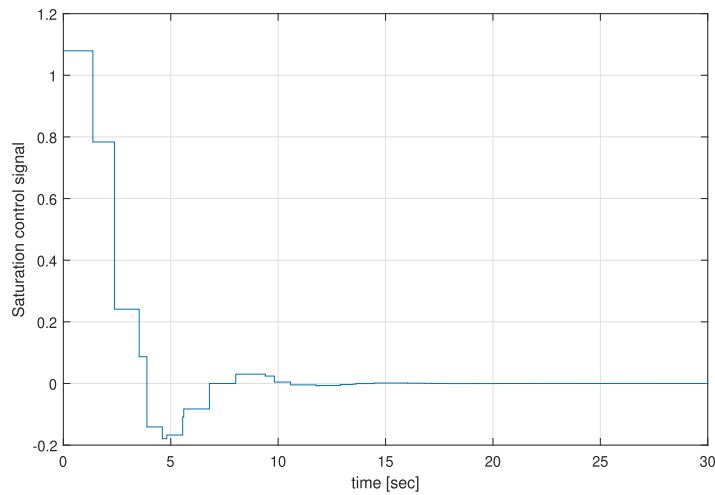


FIGURE 8 Random saturation signal $\bar{o}(\varphi) = 0.2$ with control.

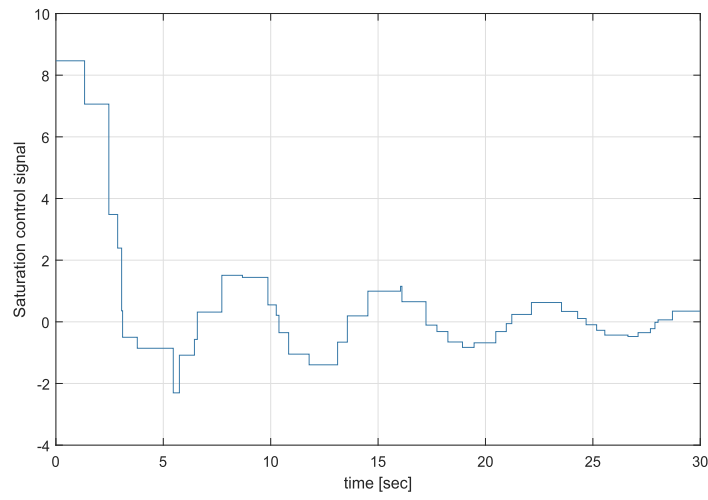


FIGURE 9 Random saturation signal $\bar{\delta}(\varphi) = 0.2$ without control.

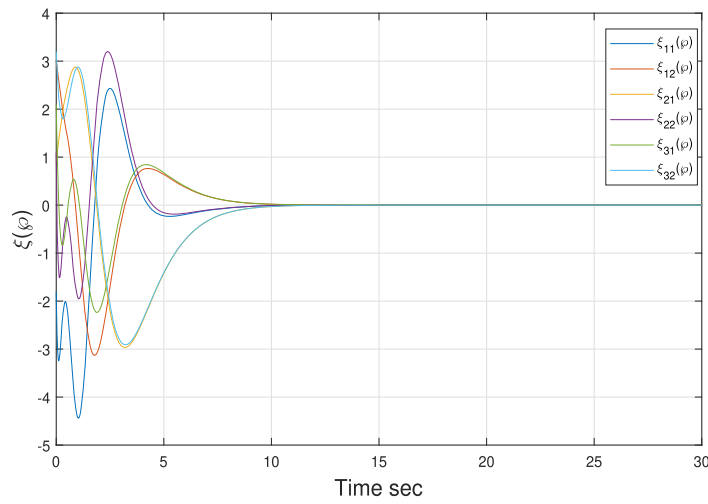


FIGURE 10 State response of the synchronization error system under deception attacks.

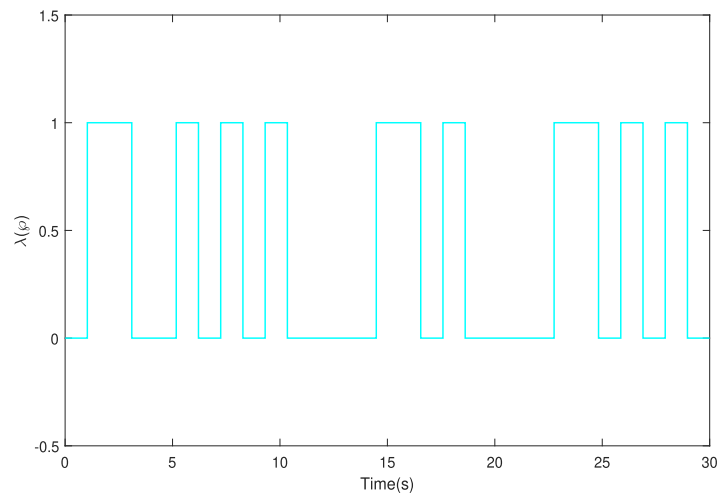


FIGURE 11 Random variable $\lambda(\varphi)$ for $\bar{\lambda} = 0.7$ (deception attacks).

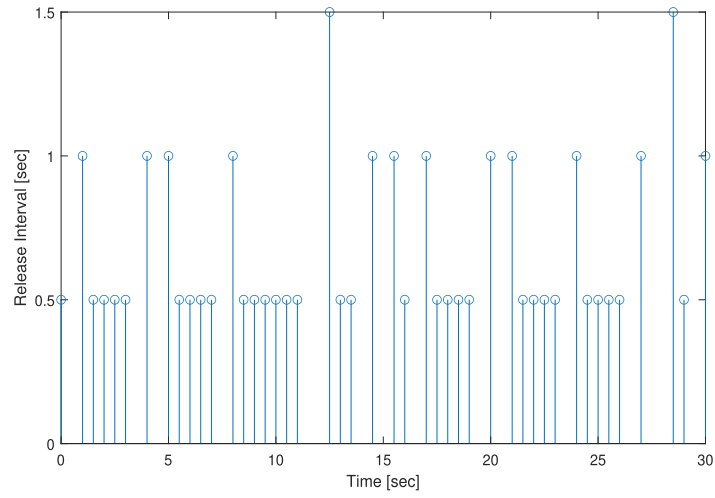


FIGURE 12 Triggered instants and released intervals.

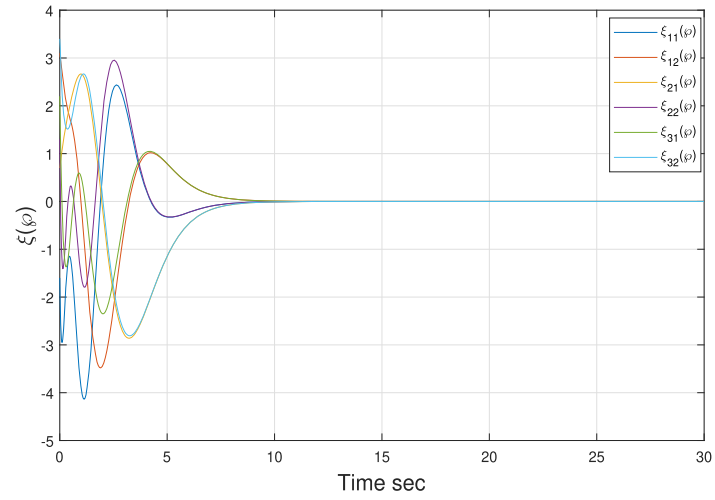


FIGURE 13 State response of the synchronization error system under replay attacks.

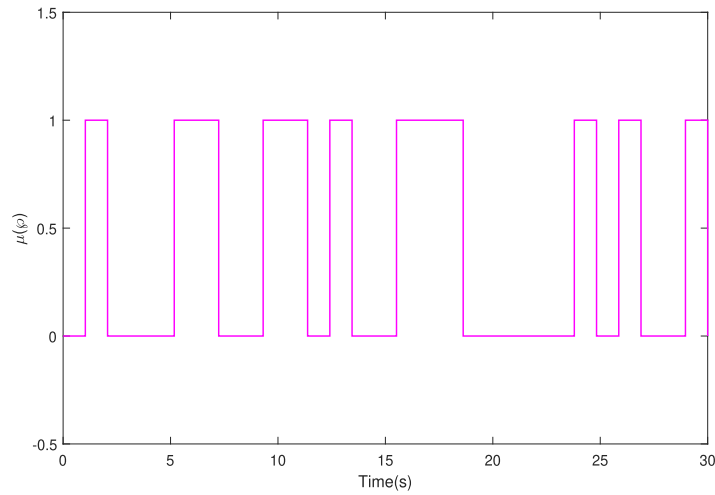


FIGURE 14 Random variable $\mu(\varphi)$ for $\bar{\mu} = 0.5$ (replay attacks).

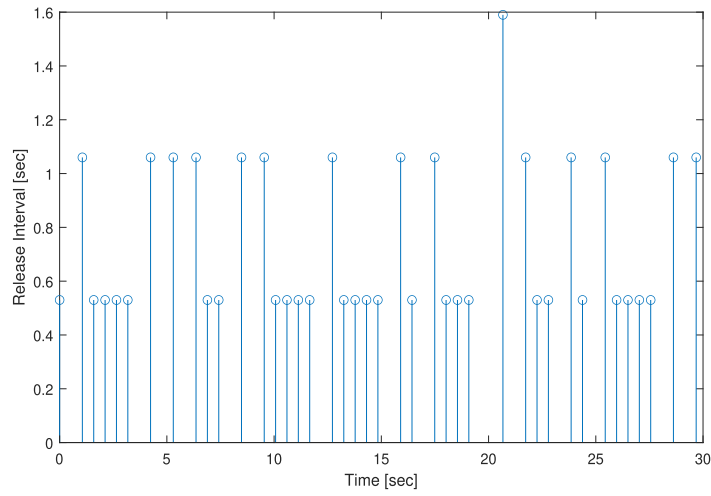


FIGURE 15 Triggered instants and released intervals.

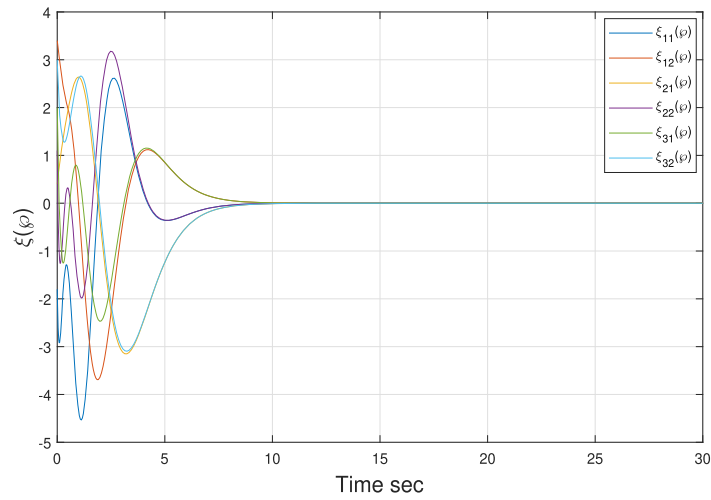


FIGURE 16 State response of the synchronization error system under DoS attacks.

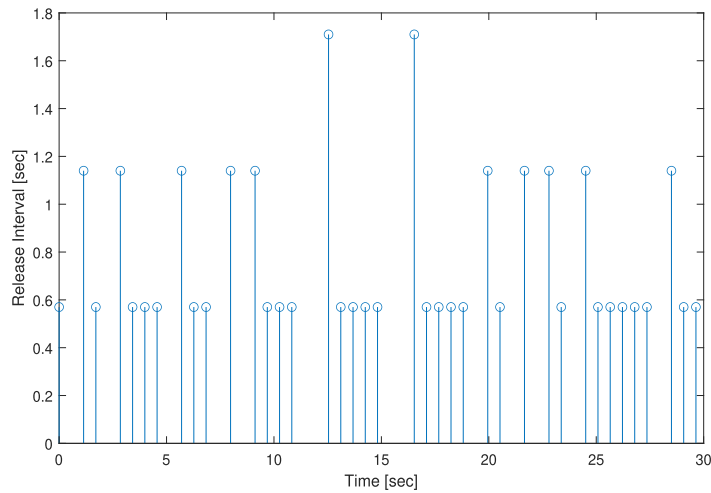


FIGURE 17 Triggered instants and released intervals.

is shown in Figure 16. It is possible to demonstrate that DoS attacks are non-periodic and satisfy Assumptions 2 and 3. The release instants and intervals are shown in Figure 17.

Remark 5. The authors discussed in different types of control for synchronization of CNs under cyber attacks.^{37,38,46} But in this work first time proposed hybrid cyber attack model for synchronization of CNs. In compared to existing work,³⁷ our results are quickly converge, where the trajectories are converges to origin within 10 s as shown in Figure 2.

5 | CONCLUSION

In this article, pinning based output synchronization control problem has been studied for CNs with random saturation under hybrid cyber-attacks via an AETS is examined. A novel hybrid cyber-attacks such as Deception, replay, and DoS attacks are first studied for synchronization of complex network. We proposed an AETS based on the adaptive law to effectively reduce the amount of unwanted data transmission in the network. Using the Lyapunov functional approach, some sufficient criteria for asymptotic stability have been obtained based on the output synchronization error system in the presence of deception attacks. Finally, a numerical example is shown to demonstrate the novelty and effectiveness of the proposed scheme. Furthermore, it is important that future research applies the proposed approach to complex modeling with a fractional order system that has a wide range of applications in real-world engineering.

ACKNOWLEDGMENTS

The financial support from the National Research Council of Thailand (Talented Mid-Career Researchers) Grant Number N42A650250.

CONFLICT OF INTEREST STATEMENT

The authors does not have any conflict of interest.

AUTHOR CONTRIBUTIONS

M. Syed Ali designed the method and manuscript preparation. M. Mubeen Tajudeen contributed significantly to analysis and manuscript preparation. Grienggrai Rajchakit contributed to the original draft, the review and edit, the funding acquisition, the formal analysis, and the conception of the study. Bandana Priya performed the experiment and data analysis, and Ganesh Kumar Thakur helped perform the analysis with constructive discussions.

ORCID

M. Syed Ali  <https://orcid.org/0000-0003-3747-3082>

REFERENCES

1. Hu T, He Z, Zhang X, Zhong S, Shi K, Zhangd Y. Adaptive fuzzy control for quasi-synchronization of uncertain complex dynamical networks with time-varying topology via event-triggered communication strategy. *Inform Sci.* 2022;582:704-724.
2. Wang Y, Hu X, Shi K, Song X, Shen H. Network-based passive estimation for switched complex dynamical networks under persistent dwell-time with limited signals. *J Franklin Inst.* 2020;3657(15):10921-10936.
3. Ali MS, Usha M, Kwon OM, Gunasekaran N, Thakur GK. H_∞ /passive non-fragile synchronization of Markovian jump stochastic complex dynamical networks with time-varying delays. *Int J Syst Sci.* 2021;52(7):1270-1283.
4. Mani P, Joo YH, Assawinchaichotec W. Fuzzy-logic-based event-triggered H_∞ control for networked systems and its application to wind turbine systems. *Inform Sci.* 2022;585:144-161.
5. Liu YA, Tang S, Liu Y, Kong Q, Wang J. Extended dissipative sliding mode control for nonlinear networked control systems via event-triggered mechanism with random uncertain measurement. *Appl Math Comput.* 2021;396:125901.
6. Gonzalez A, Cuenca A, Salt J, Jacobs J. Robust stability analysis of an energy-efficient control in a networked control system with application to unmanned ground vehicles. *Inform Sci.* 2021;578:64-84.
7. Wang H, Xie S, Zhou B, Wang W. Non-fragile robust H_∞ filtering of Takagi-Sugeno fuzzy networked control systems with sensor failures. *Sensors.* 2020;20(1):17.
8. Hu F, Jiao C, Chang H, Su X, Gu Y. Event-triggered control for networked control system via an improved integral inequality. *J Franklin Inst.* 2021;358(5):2661-2682.
9. Pang ZH, Fan LZ, Sun J, Liu K, Liu GP. Detection of stealthy false data injection attacks against networked control systems via active data modification. *Inform Sci.* 2021;546:192-205.

10. Nagamani G, Karthik C, Joo YH. Event-triggered observer-based sliding mode control for T-S fuzzy systems via improved relaxed-based integral inequality. *J Franklin Inst.* 2020;357(14):9543-9567.
11. Li Y, Song F, Liu J, Xie X, Tian E. Decentralized event-triggered synchronization control for complex networks with non periodic DoS attacks. *Appl Math Comput.* 2022;32(3):1633-1653.
12. Liu D, Yea D. Observer-based synchronization control for complex networks against asynchronous attacks. *Inform Sci.* 2021;546:753-768.
13. Lee TH, Park JH. Design of sampled-data controllers for the synchronization of complex dynamical networks under controller attacks. *Adv Differ Equ.* 2019;2019:184.
14. Pradeep C, Cao Y, Murugesu R, Rakkiyappan R. An event-triggered synchronization of semi-Markov jump neural networks with time-varying delays based on generalized free-weighting-matrix approach. *Math Comput Simul.* 2019;159:41-56.
15. Liu J, Gu Y, Xie X, Yue D, Park JH. Hybrid-driven-based \mathcal{E}_∞ control for networked cascade control systems with actuator saturations and stochastic cyber attacks. *IEEE Trans Syst Man Cybern Syst.* 2019;49(12):2452-2463.
16. Ali MS, Gunasekaran N, Kwon OM. Delay dependent H_∞ performance state estimation of static delayed neural networks using sampled-data control. *Neural Comput Appl.* 2018;30(2):539-550.
17. Cao Y, Maheswari K, Dharani S, Sivaranjani K. New event based H_∞ state estimation for discrete-time recurrent delayed semi-Markov jump neural networks via a novel summation inequality. *J Artif Intell Soft Comput Res.* 2022;12(3):207-221.
18. Ali MS, Vadivel R, Kwon OM. Decentralised event-triggered impulsive synchronization for semi-Markovian jump delayed neural networks with leakage delay and randomly occurring uncertainties. *Inform Sci.* 2019;50(8):1636-1660.
19. Liu J, Liu Q, Cao J, Zhang Y. Adaptive event-triggered H_∞ filtering for T-S fuzzy system with time delay. *Neurocomputing.* 2015;189:86-94.
20. Chen X, Wang Y, Hu S. Event-triggered quantized H_∞ control for networked control systems in the presence of denial-of-service jamming attacks. *Nonlinear Anal Hybrid Syst.* 2019;33:265-281.
21. Ali MS, Vadivel R, Kwon OM, Murugan K. Event triggered finite time H_2 Boundedness of uncertain Markov jump neural networks with distributed time varying delays. *Neural Process Lett.* 2019;49:1649-1680.
22. Cao L, Li H, Wang N, Zhou Q. Observer-based event-triggered adaptive decentralized fuzzy control for nonlinear large-scale systems. *IEEE Trans Fuzzy Syst.* 2019;27(6):1201-1214.
23. Syed Ali M, Vadivel R, Alsaedi A, Ahmad B. Extended dissipativity and event-triggered synchronization for T-S fuzzy Markovian jumping delayed stochastic neural networks with leakage delays via fault-tolerant control. *Soft Comput.* 2020;24:3675-3694.
24. Ali MS, Vadivel R, Kwon OM. Decentralized event-triggered stability analysis of neutral-type BAM neural networks with Markovian jump parameters and mixed time varying delays. *Int J Control Autom Syst.* 2018;16:983-993.
25. Li M, Zhao J, Xia J, Zhuang G, Zhang W. Extended dissipative analysis and synthesis for network control systems with an event-triggered scheme. *Neurocomputing.* 2018;312(27):34-40.
26. Kazemy A, Lam J, Chang Z. Adaptive event-triggered mechanism for networked control systems under deception attacks with uncertain occurring probability. *Int J Syst Sci.* 2021;52(7):1426-1439.
27. Pan R, Tana Y, Du D, Fei S. Adaptive event-triggered synchronization control for complex networks with quantization and cyber-attacks. *Neurocomputing.* 2020;382:249-258.
28. Xie W, Zhu Q. Input-to-state stability of stochastic nonlinear fuzzy Cohen-Grossberg neural networks with the event-triggered control. *Int J Control.* 2020;93(9):2043-2052.
29. Ratnavelu K, Kalpana M, Balasubramaniam P. Stability analysis of fuzzy genetic regulatory networks with various time delays. *Bull Malays Math Sci Soc.* 2018;41:491-505.
30. Qi Y, Zhao X, Huang J. H_∞ filtering for switched systems subject to stochastic cyber attacks: a double adaptive storage event-triggering communication. *Appl Math Comput.* 2021;394:125789.
31. Zhou X, Gu Z, Yang F. Resilient event-triggered output feedback control for load frequency control systems subject to cyber attacks. *IEEE Access.* 2019;7:58951-58958.
32. Zhang L, Guo G. Observer-based adaptive event-triggered sliding mode control of saturated nonlinear networked systems with cyber-attacks. *Inform Sci.* 2021;543(8):180-201.
33. Sun L, Wang Y, Feng G. Control design for a class of affine non-linear descriptor systems with actuator saturation. *IEEE Trans Automat Contr.* 2015;60(8):2195-2200.
34. Liu J, Suo W, Xie X, Yue D, Cao J. Quantized control for a class of neural networks with adaptive event-triggered scheme and complex cyber-attacks. *Int J Robust Nonlinear Control.* 2021;31(10):4705-4728.
35. Ma YS, Che WW, Deng C. Dynamic event-triggered model-free adaptive control for nonlinear CPSs under aperiodic DoS attacks. *Inform Sci.* 2022;589:790-801.
36. Lu H, Deng Y, Xu Y, Zhou W. Event-triggered H_∞ filtering for networked systems under hybrid probability deception attacks. *IEEE Access.* 2020;8:192030-192040.
37. Zhu Y, Pan R, Tan Y, Fei S. Adaptive event-based non-fragile output pinning synchronization control for complex networks with random saturations and cyber-attacks. *IEEE Access.* 2021;9:122712-122722.
38. Ding D, Tang Z, Wang Y, Jia Z. Secure synchronization of complex networks under deception attacks against vulnerable nodes. *Appl Math Comput.* 2021;399:126017.
39. Gu Z, Park JH, Yue D, Wu ZG, Xie X. Event-triggered security output feedback control for networked interconnected systems subject to cyber-attacks. *IEEE Trans Syst Man Cybern.* 2021;51(10):6197-6206.
40. Yin T, Gu Z. Security control for adaptive event-triggered networked control systems under deception attacks. *IEEE Access.* 2021;9:10789-10796.

41. Zhao L, Yang GH. Cooperative adaptive fault-tolerant control for multi-agent systems with deception attacks. *J Franklin Inst.* 2020;357(6):3419-3433.
42. Tahoun AH, Arafaa M. Cooperative control for cyber-physical multi-agent networked control systems with unknown false data-injection and replay cyber-attacks. *ISA Trans.* 2021;110(21):1-14.
43. Peng C, Sun H. Switching-like event-triggered control for networked control systems under malicious denial of service attacks. *IEEE Trans Automat Contr.* 2020;65(9):3943-3949.
44. Liu J, Zhang N, Li Y, Xie X. H_∞ filter design for discrete-time networked systems with adaptive event-triggered mechanism and hybrid cyber attacks. *J Franklin Inst.* 2021;358(17):9325-9345.
45. Liu J, Wei L, Xie X, Tian E, Fei S. Quantized stabilization for T-S fuzzy systems with hybrid-triggered mechanism and stochastic cyber-attacks. *IEEE Trans Fuzzy Syst.* 2018;26(6):3820-3834.
46. Zhang Z, Chen Z, Sheng Z, Li D, Wang J. Static output feedback secure synchronization control for Markov jump neural networks under hybrid cyber-attacks. *Appl Math Comput.* 2022;430:127274.
47. Deng Y, Lu H, Zhou W. Security even-triggered control for Markovian jump neural network against actuator saturation and hybrid cyber attacks. *J Franklin Inst.* 2021;358:7096-7188.
48. Liu J, Wang Y, Cao J, Yue D, Xie X. Secure adaptive-event-triggered filter design with input constraint and hybrid cyber attack. *IEEE Trans Cybern.* 2021;51(8):4000-4010.

How to cite this article: Ali MS, Tajudeen MM, Rajchakit G, Priya B, Thakur GK. Adaptive event-triggered pinning synchronization control for complex networks with random saturation subject to hybrid cyber-attacks. *Int J Adapt Control Signal Process.* 2023;1-22. doi: 10.1002/acs.3625